LBNL 49293

ERNEST ORLANDO LAWRENCE
BERKELEY NATIONAL LABORATORY

Laboratory Study of Pressure Losses in Residential Air Distribution Systems

B. Abushakra, D.J. Dickerhoff, I.S. Walker and M.H. Sherman

Environmental Energy

Technologies Division

December 2001

This work was funded by Pacific Gas and Electric Company under Contract S9902A, to support PG&E's energy efficiency programs in new and existing residential buildings via the California Institute for Energy Efficiency under Contract No. S9902A. This work was also supported by the Assistant Secretary for Energy Efficiency and Renewable Energy, Office of Building Technology, State and Community Programs, Office of Building Research and Standards, of the U.S. Department of Energy under Contract No. DE-AC03-76SF00098.

Disclaimer

Laboratory Study of Pressure Losses in Residential Air Distribution Systems

TABLE OF CONTENTS

EXECUTIVE SUMMARY

An experimental study was conducted to evaluate the pressure drop of residential duct system components that are either not available or poorly described in existing duct design literature (for instance, ASHRAE Fundamentals, and ACCA Manual D). The tests were designed to examine cases normally found in typical residential and light commercial installations. The study was divided in two parts: a component analysis and an installed system analysis. The component analysis included three different sizes of flexible ducts under different compression configurations and different bending angles, splitter boxes, supply boots, and a fresh air intake hood. The experimental tests followed the proposed ASHRAE Standard 120P – Methods of Testing to Determine Flow Resistance of HVAC Air Ducts and Fittings. The installed system analysis included the calculation of total pressure drop in the supply section of a typical residential air distribution system, based on the pressure drop results from the component analysis. The component analysis results were compared with calculations based on available literature (ASHRAE Fundamentals and ACCA Manual D). All three methods were compared to measured values of supply plenum static pressure.

The flexible duct study covered compressibility and bending effects on the total pressure drop. For better quantification of the pressure drop in flexible ducts a pressure drop correction factor, PDCF, was developed that is a function of the geometry of the duct and the compression ratio. The PDCF relationship was used to predict the pressure drop in compressed ducts is within 3% compared with the measured compressed duct values. The results also showed that ASHRAE Fundamentals and ACCA Manual D underestimate the pressure drop in compressed flexible ducts. The laboratory testing suggests an improved flexible duct clamping arrangement should be used in ASHRAE Standard 120P to ensure that duct compression is correct.

In addition to compression of straight ducts, the pressure drop in bent flexible ducts was also measured. Flexible duct of three different diameters were each tested at three bending angles. Each of the bending configurations was tested with the duct under moderate and extreme compression (around 5% and 30% compression ratios, respectively). The loss coefficients varied over a wide range between 0.8 and 3. Published loss coefficients for sheet metal elbows are about one fourth of these values, indicating that the flexible ducts have significantly greater flow resistance.

The supply boots results showed that diffusers have a major effect on the pressure losses in exit fittings. The diffuser can increase the pressure drop by factors between 1.1 and 2.0, depending on the configuration of the boot connection. For example, for an Angle Supply boot with an 8” intake the loss coefficient is 1.2 without diffuser and 2.4 with diffuser. This study included additional configurations commonly found in duct systems, where a section of bent flexible duct is attached to the boot. In such configurations, the pressure drop increased by factors between 3 and 4, compared with the values obtained when the boot is connected to a straight sheet metal duct.

Three sizes of splitter boxes were tested. The results showed that the local loss coefficient through a branch of the splitter box could vary between 0.6 and 6.3 depending on geometry and flow ratios. A typical result is 1.0 and 1.5 for the smaller and the larger branch of a 10”x8”x6” splitter box, respectively, when the flow is balanced. ASHRAE Fundamentals shows local loss coefficients values for rectangular “Tee’s” and “Wye’s” that cover the range of the results obtained in this study. ASHRAE Fundamentals does not show data for splitter boxes. ACCA Manual D provides pressure drop for splitter boxes in terms of equivalent length (EL) that overestimates the pressure drop in splitter boxes compared to our experimental data.

Lastly, an outside air intake hood was tested. The local loss coefficient of the intake hood was 4.1. This is in the middle of the range of ASHRAE loss estimates determined by combining the ASHRAE loss coefficient for a flush entry and for a screen.

The complete duct system analysis consisted of calculating the total pressure drop in the supply section of the air distribution system, based on the pressure drop results from the

component analysis. The calculated values were compared to measured values from a full-scale residential duct system constructed in an LBNL duct testing facility, and values from ASHRAE and ACCA. The installed system had two supply plenum take-offs serving two separate supply branches with a total of 11 supply registers. The measured supply plenum static pressure varied between 0.130 and 0.168 in water (depending on the location of the static pressure tap), while the calculated static pressure at the entry of the two branches (from the supply plenum), based on the component analysis, were 0.122 and 0.168 in water. The ACCA Manual D calculations overpredict the pressure drop for splitter boxes while underpredicting for the flexible duct and the supply boots. Conversely, the ASHRAE component values underpredict the pressure drop in both the flexible duct and the duct fittings.

INTRODUCTION

Evaluation of residential HVAC system performance requires estimates and measurements of several characteristic parameters. The installation of air distribution systems and the type of duct fittings used play a major role in the overall system performance. The flow resistance of each component of the air distribution system, and its specific installation configuration should be available and well known for the designer. For instance, plastic flexible ducts are commonly used in the residential building sector, while they are poorly represented in the literature. It is crucial for the designer and the contractor to realize the impact pressure drop in flexible ducts can have on the fan sizing and on the overall performance of the HVAC system. The available literature also lacks sufficient description of loss coefficients for other commonly used residential duct fittings such as, splitter boxes, outside air intake hoods and air supply boots.

Laboratory testing and a detailed analysis of air flow and resistance were conducted by the Energy Performance of Buildings Group at LBNL to identify key aspects of the performance of air distribution systems with commonly used fittings so that these systems can be improved in both new construction and retrofits of existing buildings. The analysis was divided in two parts, the *component analysis* and the *complete duct system analysis*. A new complete full-scale residential air distribution system testing facility was built to perform the *complete duct system analysis*. The laboratory measurements allowed the evaluation of the flow resistance parameters of duct fittings under controlled conditions following standard procedures (ASHRAE Standard 120P), in addition to the performance of a controlled and complete full-scale air distribution system.

This report describes the tests performed and shows the results that help as new data for residential duct design. The report first discusses the instrumentation of the test apparatus, then covers the description and the results of the individual tests on the duct components, and the analysis of the whole ducting system, as installed. The results on the tested air distribution system components were used in the complete duct system analysis and compared with available data from the literature. The comparison showed that our new data provide a better estimation of the total pressure drop. The report also includes a detailed study of the compression effects on pressure losses in flexible ducts, and proposes a new semiempirical model to calculate the pressure drop in flexible ducts.

DESCRIPTION OF THE TEST FACILITY

The tests were conducted in two duct testing laboratories at LBNL in Berkeley, CA. The smaller laboratory is a single story trailer that is used for calibration and fabrication of air flow and thermal diagnostic equipment. The larger laboratory is part of a warehouse facility that has large open areas suitable for laying out large quantities of ducting. The individual component tests were conducted in both facilities, with the larger facility used for the flex duct compression tests that required long straight lengths of duct. This larger facility also contained a full size residential duct system typical of those found in California houses.

Test Ducts and Fittings

The air distribution system components tested for this project included flexible duct, splitter boxes, supply boots, and an outside air intake hood. The flexible duct tests included three sizes of duct: 6”, 8”, and 10” (150, 200, 250 mm). The flexible duct was tested with three compression configurations: fully stretched, a natural stretch configuration, and compressed. These compression values are somewhat arbitrary, but the rationale for the selected values was as follows: the fully stretched has the inner core of the flex duct pulled tight resulting in a relatively smooth inner duct surface. For the natural stretch case no attempt was made to stretch out the duct. The compressed case represents an approximation to field observations of installed duct where the compression is mechanically enforced. Additional configurations were also tested as the flexible duct forms an elbow. Three elbow angles were tested: 45^{o}, 90^{o}, and 135^{o}. Each of

the elbow configurations included a natural stretch and a compressed configuration. The total number of flexible duct tests conducted for each duct size was nine, totaling 27 tests for all three duct sizes. The splitter boxes tests included three sizes: 8”x6”x6”, 10”x8”x6”, and 10”x8”x8” (200x150x150 mm, 250x200x150 mm, and 250x200x200 mm). The supply boots tests included an 8” (200 mm) angle supply boot, and 8” (200 mm) and 6” (150 mm) straight supply boots. Since the angle supply boot can only be connected with a horizontally spanning duct, it was tested in a single configuration as required by the ASHRAE Standard (ASHRAE 1995). However, the 8” (200 mm) and the 6” (150 mm) straight supply boots were tested under three different configurations each. The straight supply boot is usually connected, when installed, to a flexible duct forming an elbow (from a horizontal span to a vertical supply). Thus two configurations, where the bent flexible duct makes an integral part of the boot, were added to the standard configuration of testing a supply boot. Figure 1 shows two configurations of the straight supply boot tests.

Figure 1. *The 8” Straight Supply Boot tested under different configurations: a straight entry, and a right angle entry with the flexible duct as an integral part of the boot.*

Each of the supply boot tests configurations was performed without a diffuser and with a diffuser added to assess the additional pressure drop that can be encountered in an actual installation. Thus a total number of 14 tests were conducted to study the supply boots.

Test Equipment and Apparatus

The test procedures were based on proposed ASHRAE Standard 120P and involved: building piezometers of three different sizes (6”, 8”, and 10” (150 mm, 200 mm, and 250 mm)), using different lengths of sheet metal duct sections installed upstream and downstream of the test specimens, air moving fans, air flow measuring devices, and data loggers and hand-held manometers.

As required by ASHRAE Standard 120P, piezometer rings, the same diameter as the test ducts, were used that each have four equidistant static pressure taps (illustrated in Figure 2) for upstream and downstream pressure measurements. The piezometers were held by sections of sheet metal duct. The piezometer rings were made with PVC rings held in place around the sheet metal duct. The four equidistant pressure taps were manifolded together with equal lengths of flexible tubing for pressure averaging. ASHRAE Standard 120P requires that the difference between an average reading of all taps and an individual reading sensed by a single pressure tap be less than 2%. Our calibration of the pressure taps used 15 seconds readings and achieved a difference less than 2% in all cases, and it was well below 1% in most cases.

Air temperatures during the tests were stable, but a correction for temperature change during the tests was applied to all the data. The tests were conducted following proposed ASHRAE Standard 120P – Methods of Testing to Determine Flow Resistance of HVAC Air

Ducts and Fittings – December 1995. The experimental results were corrected for temperature changes during the test and for changes in flowmeter calibrations with temperature. Also elevation corrections were made because some of the tests were performed at sea level and others at several hundred feet elevation. Standard correction procedures were used as found in ASTM E779 (1999).

Figure 2. *A piezometer built for a balanced average static pressure reading and used in the component analysis tests.*

The tests required using sections of sheet metal duct upstream and downstream of the test specimen that hold the pressure tap piezometers. The piezometers were located at 2 diameters upstream and downstream of the flexible duct test section, 2 diameters upstream and 11 diameters downstream of the splitter boxes, 2 diameters upstream of the supply boots, and 11 diameters downstream of the intake hood. The total pressure drop between the upstream and downstream piezometers therefore includes the drop through the sheet metal duct, which should be subtracted from the total. Therefore the first task in the study was to characterize the pressure drop in the sheet metal duct as a function of the volumetric flow rate. The power law model (Equation 1) was used that allows for variations (for instance, due to boundary layer development or Reynolds Number effects) from the standard assumption of volumetric flow rate being proportional to the square root of the pressure drop:

$$\Delta P = CQ^n \qquad (1)$$

The results of the sheet metal duct are shown in Table 1. The pressure drop coefficient, *C*, is expressed in *in water/100ft.cfm*^{n} (Pa s^n/m.L^n), because pressure drop per 100ft is a standard unit used in existing design calculation procedures.

TABLE 1. Power Law Coefficients of Three Sizes of Sheet Metal Duct and Comparison with Resulting Pressure Drop with Available References.

Diameter in (mm)	C in water/ 100 ft. cfm^n (Pa.s^n/m.L^n)	Lower 95% CL of C in water/ 100ft. cfm^n (Pa.s^n/m.L^n)	Upper 95% CL of C in water/ 100ft. cfm^n (Pa.s^n/m.L^n)	n	Lower 95% CL of n	Upper 95% CL of n	ASHRAE Pressure Drop Average Over/Under-prediction
6 (150)	2.54 E-05 (4.40 E-04)	2.38 E-05 (4.11 E-04)	2.72 E-05 (4.72 E-04)	1.77	1.75	1.78	0.15%
8 (200)	5.99 E-06 (1.04 E-04)	4.86 E-06 (8.42 E-05)	7.37 E-06 (1.28 E-04)	1.81	1.77	1.84	-2.85%
10 (250)	3.03 E-06 (5.25 E-05)	1.62 E-06 (2.81 E-05)	5.66 E-06 (9.80 E-05)	1.74	1.63	1.84	-3.49%

Air flows were measured using either a 6" (150 mm) nozzle flowmeter (±0.5% of reading accuracy) or a combined fan/flowmeter device with ±3% accuracy. Flow straighteners that reduce swirl and turbulence were incorporated into the experimental apparatus and the flow meters. For the splitter box tests a fan/flowmeter was mounted on each downstream leg of the splitter boxes to suck air through the test system and measure the flow through each leg. The 6" (150 mm) nozzle flowmeter was used to measure the total air flow through the main branch upstream of the splitter box. All pressure and flow measurements were averaged for five seconds and the readings were recorded using a data logger. In addition to the data loggers, hand-held electronic digital pressure gauges were used in the supply boot and the splitter box tests to modulate different pressure/flow stations.

AIR DISTRIBUTION SYSTEM COMPONENT ANALYSIS

The first part of the study was to conduct a component analysis of a residential air distribution system that covered a detailed pressure drop study of flexible duct and provided a list of pressure loss coefficients of various duct fittings. The results of the component analysis were compared with available references, whenever a similar duct fitting was reported in the literature. A further evaluation of the components analysis results was performed through a comparison with measured pressure drop in an installed air distribution system (discussed in a separate section).

Effect of Compression on Pressure Loss in Flexible Ducts

Three different sizes of ducts, of 6", 8" and 10" (150, 200 and 250 mm) nominal diameters were tested under different compression configurations following proposed ASHRAE Standard 120P "Methods of Testing to Determine Flow Resistance of HVAC Air Ducts and Fittings"(December 1995). The flexible duct consists of three layers: (1) outer plastic layer, (2) R-4.2 (RSI-0.74 m^2K/W) fiberglass insulation, and (3) inner liner which is a thin plastic layer with embedded spiral wire.

In field studies observed pressure drops in flexible duct systems are often higher than expected based on design calculations. This is because the flexible ducts are often found to be compressed to varying degrees. This common problem leads to excessive pressure drop in many systems with associated fan power, flow restriction and noise issues. For design purposes and for diagnosing duct systems, engineers and analysts consult friction charts and matching friction loss coefficients from references. For fully stretched flexible duct, in particular, ASHRAE Fundamentals (ASHRAE 2001) and ACCA Manual D (ACCA 1995) provide pressure drop calculations.

However, when it comes to the compression effects on flexible ducts, the available literature does not provide enough resources for a good estimate of pressure drop in a duct

system. ASHRAE Fundamentals provides a graph, (reproduced in Figure 3), showing how compressing a fully stretched flexible duct increases the pressure drop. This single graph is used for all sizes of flexible ducts, and there is no friction chart provided.

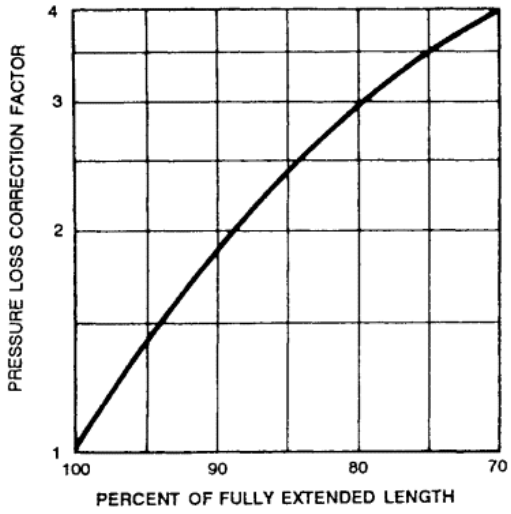

Figure 3. *ASHRAE Fundamentals 2001 (Figure 8, p.34.8) correction factor for unextended flexible duct. Copyright 2001, American Society of Heating, Refrigerating and Air-Conditioning Engineers, Inc. 1791 Tullie Circle, NE, Atlanta, GA 30329, 404-636-8400, www.ashrae.org. Reprinted by permission from 2001 ASHRAE Handbook – Fundamentals.*

ASHRAE Fundamentals (Chapter 34, *Duct Design*) suggests the use of the friction loss equation (Equation 2) with the Altshul-Tsal equation of friction factor (Equation 3) (Altshul and Kiselev 1975, and Tsal 1989), for the calculation of pressure drop in flexible ducts:

$$\text{IP:}\quad \Delta P_f = \frac{12\,fL}{D}\rho\left(\frac{V}{1097}\right)^2$$

$$\text{SI:}\quad \Delta P_f = \frac{fL}{D}\rho\frac{V^2}{2} \qquad (2)$$

$$\text{IP:}\quad f' = 0.11\left(\frac{12\varepsilon}{D}+\frac{68}{Re}\right)^{0.25}$$

$$\text{SI:}\quad f' = 0.11\left(\frac{\varepsilon}{D}+\frac{68}{Re}\right)^{0.25} \qquad (3)$$

$$\text{If } f' \geq 0.018: \quad f = f'$$

$$\text{If } f' < 0.018: \quad f = 0.85\,f' + 0.0028$$

The problem with using the above equations is in estimating the correct value of the absolute roughness, ε, because roughness data for flexible ducts are generally not available. ASHRAE Fundamentals categorizes the roughness in five categories (smooth, medium-smooth, average, medium-rough, and rough) and provides a general absolute roughness value for each

category. It also provides a range for the roughness of each type of duct in each category. Flexible duct, "all types of fabric and wire", is considered medium-rough to rough, with an absolute roughness range of 0.0035-0.015 ft (1.0-4.6 mm) when fully extended.

When the flexible duct is compressed, the inner gets crumpled and the effective surface roughness increases orders of magnitude above the range provided in ASHRAE Fundamentals. Equation 3 is not applicable to the high roughness region (on a Moody chart) where the friction factor becomes independent of the Reynolds Number (i.e., with typical *Re* ranges encountered in an HVAC ducting system; $2x10^4<Re<5x10^4$). In this case, another model for fully-rough flow regime in pipes (ducts) found in ASHRAE Fundamentals Chapter 2 (*Fluid Flow*) (ASHRAE 2001) is more appropriate:

$$\frac{1}{\sqrt{f}} = 1.14 + 2\log\left(\frac{D}{\varepsilon}\right) \tag{4}$$

For the designer, even using an appropriate model for the friction factor and surface roughness, such as in Equation 4, would be problematic, since having the appropriate value of the roughness for the specific compression case of the flexible duct is not available.

ACCA Manual D (ACCA 1995) provides a friction chart for flexible, spiral wire helix core ducts. There are conditions for using the chart, such as maximum air velocity and temperature and positive and negative pressure, but there is no indication of whether the chart was established for "fully extended" ducts.

Experimental Study

Figure 4 shows the test apparatus used in all the flexible duct tests. The test apparatus included an upstream nozzle flowmeter, entry and exit straight sheet metal duct pieces holding the upstream and downstream piezometers, and a flexible connection to the fan. A flow straightener was added at the entry of the nozzle flowmeter. Each piezometer had four equidistant pressure taps the readings of which were averaged for a single reading. The fan was equipped with a damper to modulate the flow. The flexible duct was taped to the laboratory floor to ensure a straight layout. This is of particular concern when the duct is compressed, because it tends to bulge under compression.

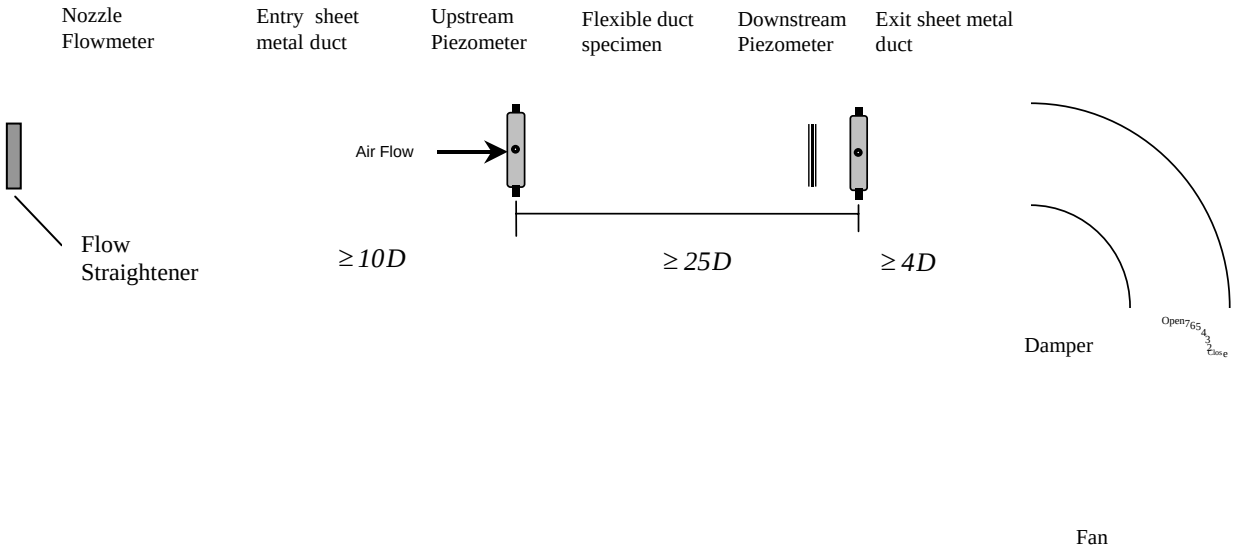

Figure 4. *Schematic of the flexible duct testing apparatus.*

Testing Fully Stretched Flexible Duct

Fully stretched (FS) flexible ducts were tested first in order to establish a baseline. The fully stretched specimen length was at least 35 diameters, satisfying the minimum 25-diameter-length suggested by Standard 120P for fully developed flow. A 35-diameter-length specimen can be compressed by as much as 30% and still satisfy the 25-diameter overall length constraint. Nevertheless, even with a 25-diameters-length specimen, part of the duct will experience a developing flow; for instance, at the attachments to the sheet metal duct carrying the piezometers upstream and downstream of the flexible duct specimen. Allowing the flow exponent of the power law model (pressure drop vs. volumetric flow rate) to vary in the analysis of the results can account for effects of these developing flow regions on pressure drop.

Because we followed the ASHRAE Standard 120P for conducting our tests, we applied its "Annex E - Flexible Duct Setup Guide" stating that "……Two wraps of duct tape and a clamp shall be used to secure the test duct connections and make an airtight connection". When a specimen is cut to length, the outer layer and the insulation lengths do not correspond, necessarily, to a fully stretched inner liner. Thus clamping the whole flexible duct (its three layers), as required by ASHRAE Standard 120P, on the inlet and outlet straight sections of rigid duct (where the piezometers are placed) could cause a situation where the outer layers are fully stretched, and the inner liner is not. For example, in one 8" (200 mm) diameter duct sample that we tested, we experienced such a situation in which the so-called "fully stretched" duct was found to be 4% compressed. The standard test procedure should be revised to require a tight connection of the inner liner only, of the test specimen, with enough duct tape to the rigid duct, without clamping the outer layers (insulation and outer plastic sheet).

Testing Compressed Flexible Duct

Tests also covered compressed flexible ducts. The compression ratios are calculated relative to the fully stretched case. The compression ratio is the change in length divided by the fully stretched length. A maximum compression ratio of 30% was achieved for the three duct sizes. Above this compression ratio, it was not possible to keep the compressed specimen straight, because it would bulge somewhere between the upstream and downstream piezometers. This bulging is caused by restrictions due to the outer liner and the insulation of the flexible duct.

In our tests, a compression of around 15% was used as a moderate compression case typically found in field installation and represents a “Normal Stretch” flexible duct scenario. A compression of around 30% would be an extreme compression case and represents a “Compressed” flexible duct scenario. Figure 5 shows the test specimen of the fully stretched 10” (250 mm) duct, and Figure 6 shows the test specimen of the compressed 10” (250 mm) duct.

Figure 5. *The fully stretched 10” (250 mm) flexible duct test specimen.*

Figure 6. *The compressed 10” (250 mm) flexible duct test specimen.*

Results

The tests for each duct size and compression configuration were conducted by recording the values of the volumetric flow rate and pressure drop in the test specimen. Every data point (volumetric flow rate and pressure drop) used in the analysis was an average of 60 five-second readings. The 60 values for each data point used in the analysis were taken after reaching a steady state flow conditions. The pressure drop in the flexible duct specimen was corrected for

the pressure drop in the straight sheet metal duct section (holding the piezometers upstream and downstream). The volumetric flow rate ranges were chosen to represent ranges that are encountered in real buildings. Table 2 summarizes the flow condition ranges achieved in the tests together with the actual and target compression ratios.

TABLE 2. Flow Conditions Ranges in the Flexible Duct Study.

Nominal Diameter in (mm)	Compression Scenario	Target Compression Ratio r_c	Actual Compression Ratio r_c	Corrected Volumetric Flow Rate cfm (L/s)	Pressure Drop in water/100ft (Pa/m)	Velocity fpm (m/s)	Reynolds Number Range
6 (150)	Fully Stretched	0.00	0.00	90 – 430 (41 – 202)	0.08 – 1.98 (0.7 – 16.2)	447 – 2176 (2.3 – 11.1)	24,000 – 115,000
	Natural Stretch	0.15	0.138	80 – 400 (38 – 189)	0.30 – 6.63 (2.5 – 54.2)	415 – 2040 (2.1 – 10.4)	22,000 – 108,000
	Compressed	0.30	0.286	90 – 390 (41 – 182)	0.72 – 12.36 (5.9 – 101.0)	439 – 1966 (2.2 – 10.0)	23,000 – 104,000
8 (200)	Fully Stretched	0.00	0.00	110 – 480 (50 – 225)	0.02 – 0.41 (0.2 – 3.4)	303 – 1364 (1.5 – 6.9)	21,000 – 97,000
	Natural Stretch	0.15	0.146	100 – 470 (48 – 221)	0.08 – 1.65 (0.7 – 13.5)	292 – 1340 (1.5 – 6.8)	21,000 – 95,000
	Compressed	0.30	0.238	110 – 470 (54 – 220)	0.16 – 2.46 (1.32– 20.1)	326 – 1333 (1.7 – 6.8)	23,000 – 94,000
10 (250)	Fully Stretched	0.00	0.00	150 – 450 (73 – 211)	0.02 – 0.14 (0.1 – 1.2)	282 – 821 (1.4 – 4.2)	25,000 – 73,000
	Natural Stretch	0.15	0.14.8	130 – 450 (63 – 213)	0.04 – 0.48 (0.4 – 3.9)	247 – 826 (1.3 – 4.2)	22,000 – 73,000
	Compressed	0.30	0.295	130 – 460 (62 – 217)	0.07 – 0.78 (0.5 – 6.3)	240 – 843 (1.2 – 4.3)	21,000 – 75,000

The first step in the analysis was to develop the pressure drop model as a function of the volumetric flow rate. The power law model (Equation 1) was used that allows for variations (for instance, due to boundary layer development or Reynolds Number effects) from the standard assumption of volumetric flow rate being proportional to the square root of the pressure drop.

To obtain an estimate of test repeatability, the test on the 10" (250 mm) duct was performed three times with different sizes of nozzle flowmeter and different lengths of specimens. The coefficient of variation (root mean squared error divided by the mean) among repeated tests in the power law model for the fully stretched 10" duct case was 5%. Note that the tests on the 8" (200 mm) duct were repeated twice because the 8" specimen in the first fully stretched case was in fact compressed by 4%. The results of the experimental study are shown in Table 3, and include both the fitted coefficients and the 95% confidence limits of these coefficients. The "normal stretch" and "compressed" scenarios corresponded to a compressed specimen length of around 25 and 30 diameters.

TABLE 3. Power Law Coefficients of Three Sizes of Flexible Ducts and Comparison with Resulting Pressure Drop with Available References.

Nominal Diameter in (mm)	Compression Ratio r_c	C in water/ 100 ft. cfm^n (Pa.s^n/m.L^n)	Lower 95% CL of C in water/ 100ft. cfm^n (Pa.s^n/m.L^n)	Upper 95% CL of C in water/ 100ft. cfm^n (Pa.s^n/m.L^n)	n	Lower 95% CL of n	Upper 95% CL of n	ACCA-ASHRAE Pressure Drop* Average Over/Under-prediction
6 (150)	0	1.20 E-05 (2.08 E-04)	1.07 E-05 (1.86 E-04)	1.34 E-05 (2.33 E-04)	1.98	1.96	2.00	+11%
	0.138	6.04 E-05 (1.05 E-03)	5.27 E-05 (9.12 E-04)	6.94 E-05 (1.20 E-03)	1.94	1.92	1.97	-28%
	0.286	1.56 E-04 (2.70 E-03)	1.32 E-04 (2.29 E-03)	1.84 E-04 (3.18 E-03)	1.90	1.87	1.93	-47%
8 (200)	0	3.33 E-06 (5.76 E-05)	9.34 E-07 (1.62 E-05)	1.19 E –05 (2.06 E-04)	1.90	1.66	2.14	+39%
	0.146	8.13 E-06 (1.41 E-04)	5.69 E-06 (9.85 E-05)	1.16 E-05 (2.01 E-04)	1.99	1.92	2.06	-8%
	0.238	1.71 E-05 (2.96 E-04)	8.83 E-06 (1.53 E-04)	3.31 E-05 (5.73 E-04)	1.94	1.81	2.06	-14%
10 (250)	0	7.31 E-07 (1.27 E-05)	2.63 E-07 (4.55 E-06)	2.03 E-06 (3.52 E-05)	1.99	1.80	2.17	+13%
	0.148	2.75 E-06 (4.76 E-05)	1.97 E-06 (3.41 E-05)	3.84 E-06 (6.65 E-05)	1.98	1.92	2.04	-15%
	0.295	4.53 E-06 (7.84 E-05)	2.92 E-06 (5.06 E-05)	7.00 E-06 (1.21 E-04)	1.97	1.89	2.05	-12%

* ACCA-ASHRAE values are average values of pressure drop corresponding to the flow rates used in each test, and calculated by multiplying the look-up values in ACCA Manual D Chart 7, page A2-10 (ACCA 1995) by the correction factor in ASHRAE Fundamentals (ASHRAE 2001), Figure 8, p.34.8. For the fully stretched case (0% compression) the correction factor is 1.

The flow exponent, *n*, was close to 2 in these tests, indicating that developing flow is not a large contributor to the pressure drop. However, taking into consideration the confidence interval of all the calculated flow exponent values, in six out of nine cases (8" and 10" (200 and 250 mm) ducts), the upper limit of the confidence interval would slightly exceed the 2.0 value. The confidence intervals could have been reduced by sampling more data pairs in the test, i.e. more volumetric-flow-rate/pressure-drop stations. In our tests, we took 16 data pairs in the 6" (150 mm) duct tests, then we reduced the tests to only four data points for the 8" and 10" (200 and 250 mm) ducts, resulting in larger confidence intervals for the 8" and 10" tests. The experimental results were compared to data in ACCA Manual D (ACCA 1995). The ACCA manual provides a look-up friction chart for flexible, spiral wire helix core ducts. It was assumed that the values ACCA provides are for a fully stretched configuration (there is no explicit definition in the chart's footnote, nor in the text). Thus to compare our results with the available references, the values provided by ACCA were multiplied by the correction factors provided in ASHRAE (2001). The ACCA chart overpredicted the pressure drop for the fully stretched duct of all sizes tested, on an average, by 21%. ACCA underpredicted the pressure drop by 17% for the normal stretch cases (around 15% compression), and by 24% for the compressed cases (around 30% compression). For all tests with different compression ratios, the average underprediction is 21%. This indicates that ACCA Manual D data was probably obtained from partially compressed flexible duct. The results of compressed ducts also showed that when a flexible duct is compressed, it can have a greater pressure drop per unit length than a fully stretched duct of a smaller diameter.

A further comparison of our flexible duct results with available literature used pressure drop data reported in technical reports published by IBACOS (1995) and Kokayko et al. (1996).

IBACOS (1995) showed data for a 8" (200 mm) flexible duct. For the fully stretched case, IBACOS pressure drop data looked very close to our results (higher by only 1%). For less than fully stretched duct, IBACOS showed pressure drop data for a 10% compression case, which were 60% higher than our results. The document does not analyze the compressibility effects and does not provide a pressure drop correction factor.

However the data showed by Kokayko et al. (1996) showed many inconsistencies from one duct size to another and with our results; there was no clear trend to characterize their results (over- or underprediction). For an 8" (200) diameter fully stretched flexible duct, their pressure drop values are 105% higher than ours; for a 10% compression the values are 87% higher. For a 6" (150 mm) duct, the values are only 4% higher than our results for fully stretched, and 34% lower for 10%-compressed cases. For a 10" (250 mm) duct, the values are 63% higher than our results for fully stretched, and 11% lower for 10%-compressed cases. The document also does not show a pressure drop correction factor analysis.

Development of a Pressure Drop Correction Factor

The pressure drop correction factor (*PDCF*) is a multiplier that can be used to estimate the pressure drop in a flexible duct when less than fully stretched, based on the pressure drop of a fully stretched duct:

$$PDCF = \frac{\Delta P}{\Delta P_{FS}} \tag{5}$$

where ΔP is the pressure drop at a particular level of compression, and ΔP_{FS} is that corresponding to a fully stretched configuration. Analysis of the measured data has shown that the pressure drop correction factor, *PDCF*, is approximated well by a linear function of the compression ratio, r_c The compression ratio, r_c, is calculated from measuring the length of the test specimen, fully stretched and under compression:

$$r_c = 1 - \frac{L}{L_{FS}} \tag{6}$$

such that:

$$PDCF = 1 + ar_c \tag{7}$$

where *PDCF* would be equal to 1 (no correction) for a zero compression, and the empirical coefficient, *a*, can be obtained from the experimental data using:

$$a = \frac{\sum_{j=1}^{m}\left(\left(\frac{\sum_{i=1}^{n}\frac{\Delta P}{\Delta P_{FS}}}{n}\right) - 1\right)}{\sum_{j=1}^{m} r_c} \tag{8}$$

where,
n = number of volumetric-flow-rate/pressure-drop stations in a test,

m = number of compression cases (tests) including the fully stretched case.

Table 4 includes the values of r_c and the calculated coefficient *a* obtained from the measured data.

TABLE 4. Compression Ratios and Calculated Coefficients in the PDCF of three Flexible Duct Sizes

Diameter in (mm)	Compression Ratio r_c	Pressure Drop Correction Factor Coefficient a
6 (150)	0	25.4
	0.138	
	0.286	
8 (200)	0	21.6
	0.146	
	0.238	
10 (250)	0	16.2
	0.148	
	0.295	

Figure 7 shows the measured *PDCF* (Equation 5) for all the measured data. This figure illustrates that PDCF is relatively constant with the flow rate and only depends on the duct diameter and the compression ratio. The figure also shows the greater effect of compression on the pressure drop for smaller duct sizes.

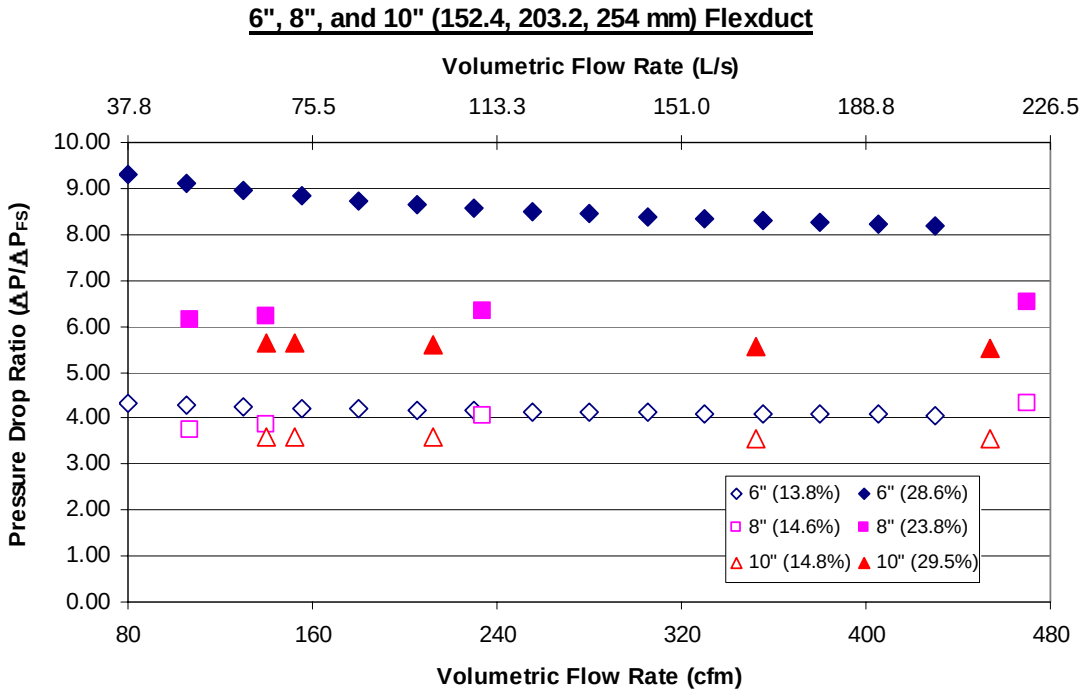

Figure 7. *The measured pressure drop ratio of normal stretch and compressed flexible duct as a function of the volumetric flow rate.*

Table 5 shows the PDCF models developed using Equation 7. A reference model, *ASHRAE-all sizes,* is also listed for comparison. This reference model was obtained with a best-fit first order polynomial ($PDCF = 1 + 9.9\ r_c$), developed from the look-up values from ASHRAE (2001) (illustrated in Figure 3). The ASHRAE model is independent of duct size and underestimates the pressure drop by an average of 35%. Figure 8 shows the corresponding *PDCF* graphs obtained using Equation 7 and the values of the coefficient *a* in Table 4. The figure also shows the individual measured PDCF values for the three duct sizes tested, and the reference ASHRAE model. Each measured PDCF value shown in the figure is an average value for all volumetric-flow-rate/pressure-drop stations for each case.

TABLE 5. Pressure Drop Correction Factor of Three Sizes of Flexible Duct

Diameter in (mm)	Pressure Drop Correction Factor PDCF
6 (150)	$1 + 25.4\ r_c$
8 (200)	$1 + 21.6\ r_c$
10 (250)	$1 + 16.2\ r_c$
ASHRAE all sizes	**$1 + 9.9\ r_c$**

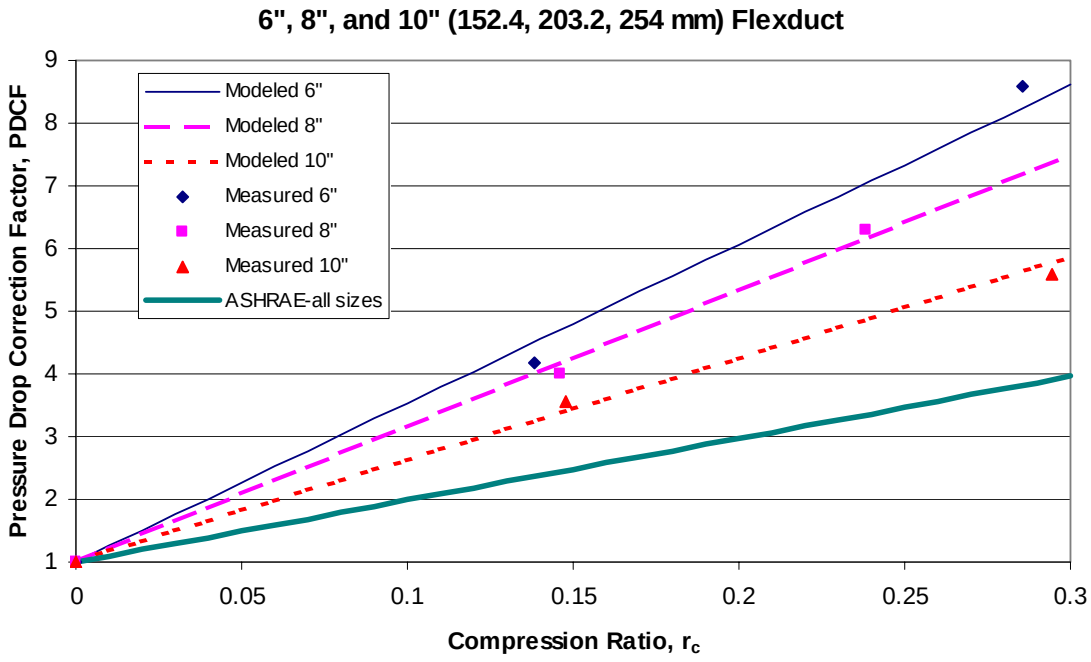

Figure 8. *Comparison of the linear pressure drop correction factor models and the ASHRAE model.*

The physical basis of the empirical relationship for the PDCF (Equation 7) can be explained in terms of change in the friction factor and the geometry of the flexible duct when compressed. Figure 9 shows a schematic of a flexible duct inner liner in fully stretched and in compressed conditions.

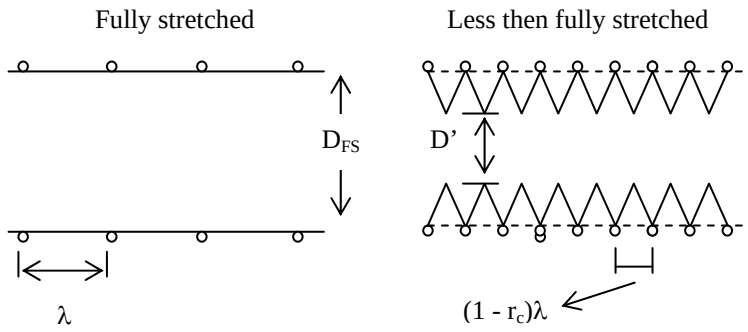

Figure 9. *Schematic of the inner liner of a flexible duct.*

Compressing the flexible duct results in a crumpled inner liner which reduces the effective interior cross-sectional area and increases its absolute surface roughness. The pitch, λ, is the distance between two consecutive spirals of flexible duct. The degree of area reduction and roughness increase depends on the pitch-to-diameter ratio (larger pitch leads to higher cross-sectional area changes and greater roughness).

Dividing the coefficient *a* in Table 4 by the corresponding pitch-to-diameter ratio of the fully stretched duct, λ_{FS}/D_{FS}, generated values that are approximately equal, indicating that it may be simple to include this duct geometry specific factor in the calculation of PDCF. This would allow the determination of PDCF for ducts not tested in this study. The average of $a/(\lambda_{FS}/D_{FS})$ for all three duct sizes was *106*. Therefore the pitch-to-diameter-normalized PDCF values use the following expression:

$$PDCF_{Norm} = 1 + 106\left(\frac{\lambda_{FS}}{D_{FS}}\right)r_c \qquad (9)$$

Figure 10 shows a comparison between the PDCF models discussed previously and those derived from $PDCF_{Norm}$. The $PDCF_{Norm}$ compared with PDCF overpredicts by an average of 4.4% for the 6" (150 mm), underpredicts by an average of 2.0% for the 8" (200 mm), and underpredicts by and average of 1.7% for the 10" (250 mm) duct. These over-and-underprediction results are within the experimental uncertainties in the power-law modeling of the measured pressure drop of compressed flexible ducts, summarized in Table 6. These small deviations indicate that this normalized model gives reasonable results and could be used to predict PDCF for other ducts of known pitch-to-diameter ratios.

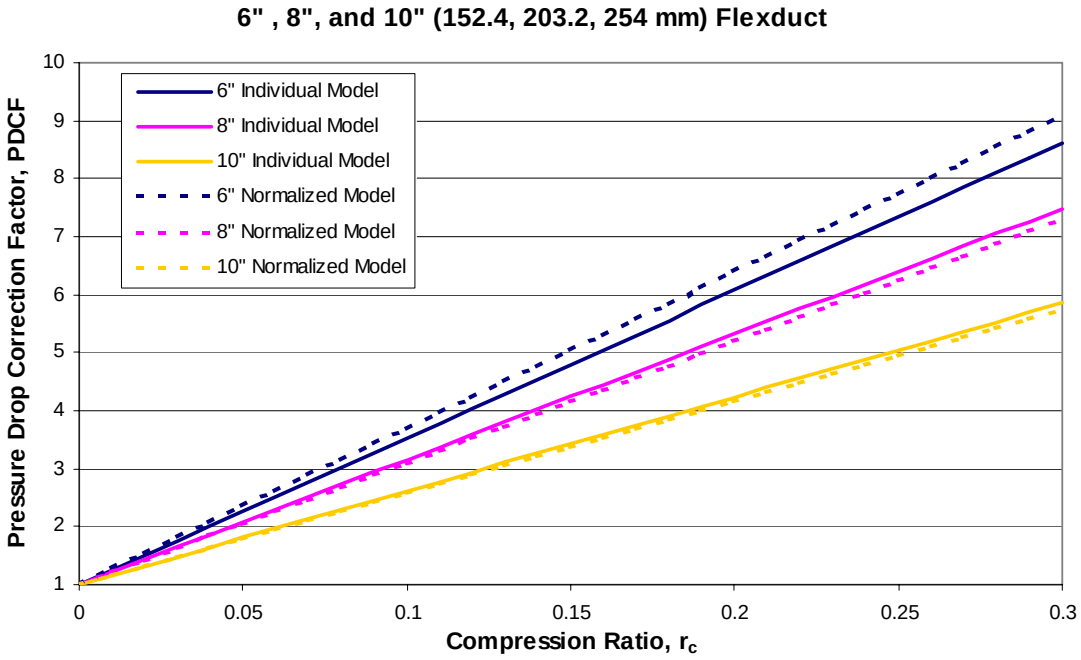

Figure 10. *Comparison between the individually calculated PDCF models (Equation 7) for each duct size and those derived from the normalized model (Equation 9).*

TABLE 6. Confidence Limits of the Power-Law Modeling of the Measured Pressure Drop for the Compressed Flexible Duct.

Duct Size in (mm)	Compression Ratio r_c	Upper 95% Confidence Limit	Lower 95% Confidence Limit
6 (150)	0.138	+5.7%	-5.4%
	0.286	+6.7%	-6.3%
8 (200)	0.146	+8.2%	-7.6%
	0.238	+13.9%	-12.2%
10 (250)	0.148	+6.5%	-6.1%
	0.295	+8.6%	-7.9%

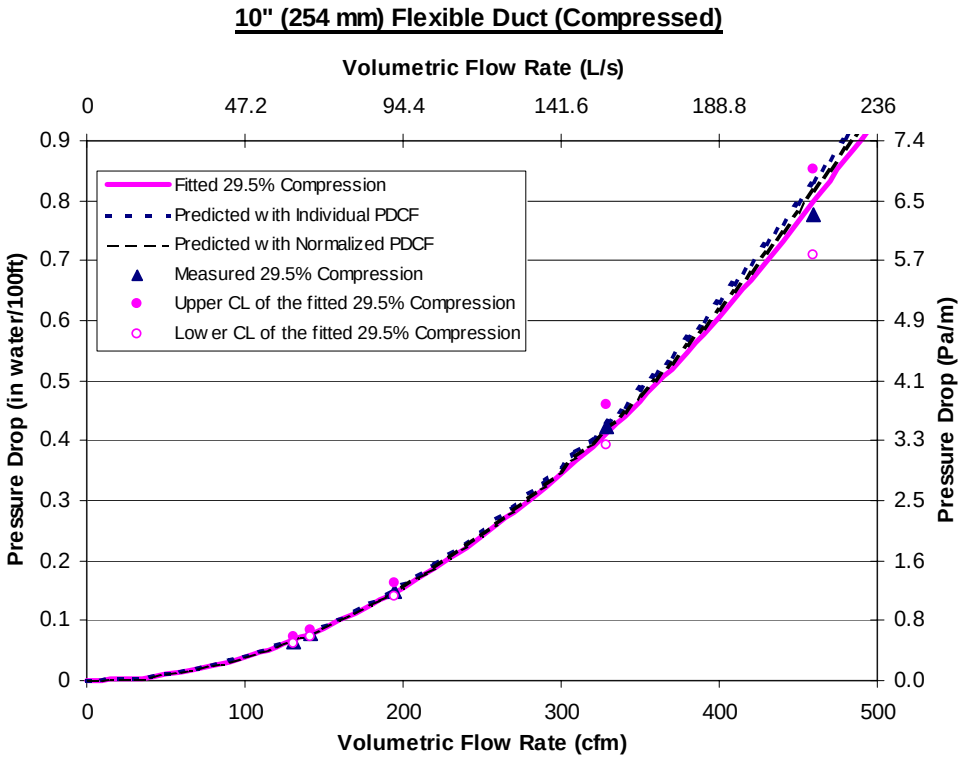

Figure 11. *Comparison between measured, power-law-fitted, and predicted pressure drop with PDCF models in a compressed 10"(250 mm) flexible duct.*

Figure 11 illustrates the pressure drop in the "compressed" 10" (250 mm) duct as measured, power-law-fitted, and predicted with two different PDCF models. The compression ratio was 29.5%, and the measured data consisted of five volumetric-flow-rate/pressure-drop stations, from which a power law model of the pressure drop was developed. The predicted pressure drop models used the power-law model developed for the fully stretched case multiplied by the pressure drop correction factor. Considering the power-law-fitted results as the basis for comparison, the model using PDCF overpredicted the pressure drop, corresponding to the measured volumetric-flow-rate, by an average of 3%, while the model using the $PDCF_{Norm}$ overpredicted the pressure drop by an average of 0.7%. Both these models give predictions that are within the experimental uncertainties.

Friction factor Approach to Compressed Flex Duct Pressure Losses

The friction factor for compressed flexible duct can be expressed in the same way as pressure drop by using an uncompressed (Fully Stretched) friction factor and friction factor correction. This correction has the same form as the PDCF:

$$f = f_{FS}\left(1 + 106\left(\frac{\lambda_{FS}}{D_{FS}}\right)r_c\right) \tag{10}$$

Figure 12 shows the calculated values of the friction factor for three duct sizes corresponding to various compression ratios using Equation 2, together with modeled data (Equation 10) that uses the calculated friction factor for fully stretched duct only. Incorporating Equation 10 into Equation 2 allows the calculation of pressure drop in terms of friction factor:

$$\text{IP:}\quad \Delta P = 12\rho\left(\frac{Q}{1097\left(\frac{\pi}{4}\left(\frac{D}{12}\right)^2\right)}\right)^2\left(\frac{L}{D}\right)\left(f_{FS}\left(1+106\left(\frac{\lambda_{FS}}{D_{FS}}\right)r_c\right)\right)$$

$$\text{SI:}\quad \Delta P = \rho\frac{\left(\frac{Q}{\left(\frac{\pi}{4}D^2\right)}\right)^2}{2}\left(\frac{L}{D}\right)\left(f_{FS}\left(1+106\left(\frac{\lambda_{FS}}{D_{FS}}\right)r_c\right)\right) \qquad (11)$$

with the air density as a function of temperature:

$$\text{IP:}\quad \rho = 0.07517\left(\frac{528}{T+460}\right)$$

$$\text{SI:}\quad \rho = 1.2041\left(\frac{293}{T+273}\right) \qquad (12)$$

Equation 12 becomes:

$$\text{IP:}\quad \Delta P = 13.3\frac{LQ^2\left(f_{FS}\left(1+106\left(\frac{\lambda_{FS}}{D_{FS}}\right)r_c\right)\right)}{D^5(T+460)}$$

$$\text{SI:}\quad \Delta P = 286\frac{LQ^2\left(f_{FS}\left(1+106\left(\frac{\lambda_{FS}}{D_{FS}}\right)r_c\right)\right)}{D^5(T+273)} \qquad (13)$$

The prediction of the pressure drops using Equation 13 were within 0.5% (on average) of the measured values, with all results within 9%. The complete comparison is summarized in Table 7.

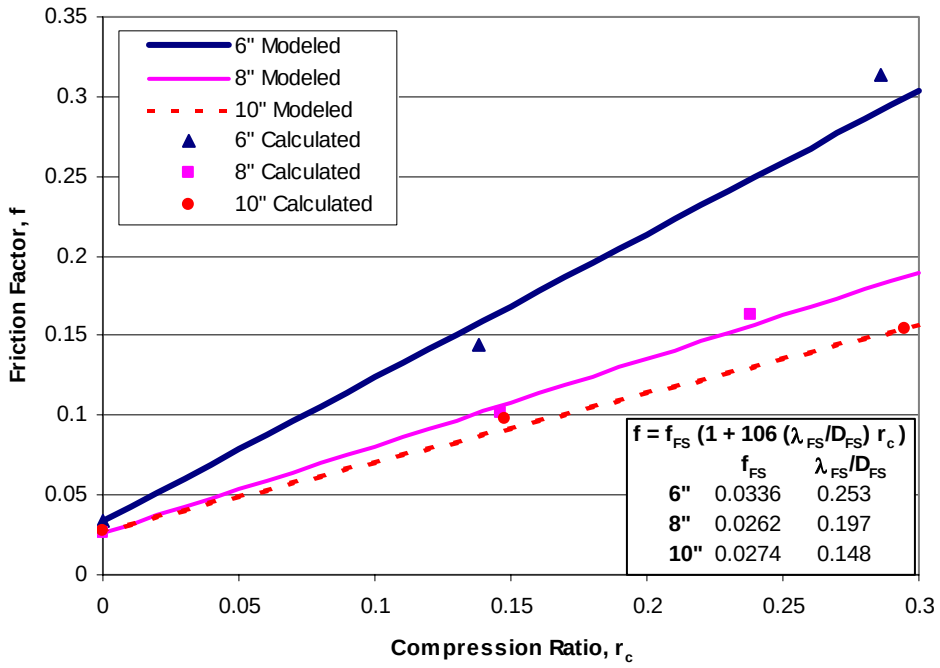

Figure 12. *Friction factor for compressed flexible ducts.*

TABLE 7. Prediction of the Pressure Drop in Three Different Sizes of Flexible Duct and Under Three Different Compression Ratios Using a Friction Factor Approach

Diameter D in (mm)	Compression Ratio r_c	λ_{FS}/D_{FS}	PDCF	Calculated Friction Factor	Length L ft (m)	Measured Pressure Drop ΔP in water (Pa)	Predicted Pressure Drop ΔP in water (Pa)	Prediction Error %
6 (150)	0	0.253	1.000	0.0336	100 (30.5)	0.061 (15.3)	0.0613 (15.3)	0.00
6 (150)	0.138	0.253	4.701	0.1579	100 (30.5)	0.265 (66.1)	0.290 (72.1)	9.13
6 (150)	0.286	0.253	8.670	0.2912	100 (30.5)	0.573 (142.6)	0.532 (132.5)	-7.09
8 (200)	0	0.197	1.000	0.0262	100 (30.5)	0.045 (11.2)	0.045 (11.2)	0.00
8 (200)	0.146	0.197	4.049	0.1059	100 (30.5)	0.174 (43.3)	0.181 (45.1)	4.13
8 (200)	0.238	0.197	5.970	0.1561	100 (30.5)	0.279 (69.6)	0.267 (66.6)	-4.30
10 (250)	0	0.148	1.000	0.0274	100 (30.5)	0.035 (8.7)	0.035 (8.7)	0.00
10 (250)	0.148	0.148	3.322	0.0912	100 (30.5)	0.124 (31.0)	0.116 (28.8)	-6.96
10 (250)	0.295	0.148	5.628	0.1545	100 (30.5)	0.195 (48.6)	0.196 (48.8)	0.42

Summary of Compressibility Effect of Flexible Duct Flow Resistance

In this study, the effect of the compression ratio on the pressure drop in flexible ducts was investigated by developing a pressure drop correction factor. The fully stretched flexible

duct was used as the baseline for all other compressed configurations. This study showed that the pressure drop (flow resistance) for flexible ducts increases significantly (by factors close to 10) when the ducts are not fully stretched. Therefore it is crucial for the designer to be aware of these compressibility effects and how the elevated pressure drop would affect the HVAC fan sizing. The contractor should also be aware of these effects, and install flexible ducts so as to reduce the compression effects. Simple pressure drop corrections factors were developed that can be applied to the pressure drop for fully stretched duct to estimate the pressure drop in compressed ducts. The results also showed that:

- A change to the standard test procedure of flexible ducts, as an improvement to ASHRAE Standard 120P, is required such that only the inner liner of the test specimen be tightly connected to the rigid duct (where the peizometers measuring the pressure drop are placed) without clamping the outer layers. This modification would insure a correct modeling of the fully stretched flexible duct pressure drop, and the derivation of accurate pressure drop correction factors for any percentage of compression.
- The correction factor suggested by ASHRAE (ASHRAE 2001) underestimates the pressure drop in all of the duct sizes tested, on an average, by 35%. In addition, the change in PDCF with duct size is not accounted for by ASHRAE.
- The friction chart provided in ACCA Manual D (ACCA 1995) overpredicts the pressure drop for fully stretched duct, on an average, by 21%. For less than fully stretched duct, ACCA values corrected with correction factors from ASHRAE Fundamentals, showed around 21% underprediction in the pressure drop.
- The pressure drop data and the PDCF models developed in this study could be used by ASHRAE and ACCA to update their handbook/manual.

Future work should focus on testing a wider range of duct sizes and ducts of the same sizes from different manufacturers to ensure that the PDCF models are generally applicable.

Bent Flexible Duct Tests

The bent flexible duct tests included the three diameter sizes analyzed in the straight layouts, with two different compression configurations; a moderate one around 5% compression and an extreme one around 30%. Three different angles for elbows were considered: 90°, 45°, and 135°. The experimental results for the bent duct tests were adjusted to account for the pressure drop in the straight duct connected to each end of the test section. The straight duct included sections of flexible duct and the sheet metal duct containing the piezometers. These sections are illustrated in Figure 13. The following corrections need to be made in order to isolate the pressure drop in the bent section of duct only.

$$\Delta P_{Elbow} = \Delta P_{1-2} - \left(L_{smd,1} + L_{smd,2}\right)\left(c_{smd} Q^{n_{smd}}\right) - \left(L_{fd,1} + L_{fd,2}\right)\left(PDCF \times c_{fd} Q^{n_{fd}}\right) \quad (14)$$

where:

ΔP_{Elbow} = Total pressure drop in the net length of the elbow
ΔP_{1-2} = Total pressure drop from upstream to downstream piezometers
$L_{smd,1}$ and $L_{smd,2}$ = Upstream and downstream lengths of the sheet metal duct sections
c_{smd} = Power law pressure coefficient of the sheet metal duct
Q = Volumetric flow rate
n_{smd} = Volumetric flow rate power law exponent of the sheet metal duct
$L_{fd,1}$ and $L_{fd,2}$ = Upstream and downstream, lengths of the straight flexible duct sections
$PDCF$ = Pressure drop correction factor
c_{fd} = Power law pressure coefficient of the fully stretched flexible duct
n_{fd} = Volumetric flow rate power law exponent of the fully stretched flexible duct

The lengths of the upstream and downstream sheet metal duct, holding the piezometers, and the straight sections of the flexible duct upstream and downstream of the bent portion of the flexible duct forming the elbow were determined following the requirements of ASHRAE Standard 120P.

After calculating the total pressure drop in the bent flexible duct section using Equation 14, the local loss coefficient of the elbow is calculated as follows:

$$K = \frac{\Delta P_{Elbow}}{P_v} \tag{15}$$

where the velocity pressure, P_v, is calculated as follows:

$$\text{IP:}\quad P_v = \rho \left(\frac{\frac{Q}{\frac{\pi}{4}\left(\frac{D}{12}\right)^2}}{1097} \right)^2$$

$$\text{SI:}\quad P_v = \rho \frac{\left(\frac{Q}{\frac{\pi}{4} D^2} \right)^2}{2} \tag{16}$$

Figure 13. *A moderately compressed (12%) 45° bent 8" (200 mm) flexible duct test specimen.*

Table 8 shows the result of the 18 tests conducted on bent flexible ducts. The loss coefficients increase with increasing turn angle, but no systematic variation can be seen. This is because of the geometry effects of varying compression ratios and the ratio of bend radius to duct diameter. The more compressed ducts do not always have higher loss coefficients for the same reason. The only similar data reported in the literature, that can be used to compare our results of the bent flexible duct were in IBACOS (1995), and in a flexible duct manufacturer "engineering

brochure". IBACOS (1995) showed the static pressure loss for 8" (200 mm) 135° and 90° elbows with three radius-to-diameter ratios. The pressure losses reported convert to local loss coefficients ranging between 2.49 and 3.93, which covers the range of our results. However the document does not discuss or report the compression scenario of the tested flexible duct elbows. On the other hand, the manufacturer brochure only showed values of local loss coefficient for a 12" (305 mm) diameter 90° elbows that ranged between 0.82 and 0.86 for radius-to-diameter ratios between 1.0 and 4.0. These results are somehow consistent with our results for smaller duct diameters (local loss coefficient decreasing as the duct diameter decreases).

Our results showed that flexible duct elbows have much higher local loss coefficients than those reported for sheet metal elbows in the literature (ASHRAE 2001). The local loss coefficients for multiple gores and pleated sheet metal elbows in ASHRAE (2001) are all below 1.0, for different angles, and *r/D* configurations of 2.5 and below. The higher loss coefficients values observed in the flexible duct elbows can be explained by the increased absolute surface roughness of the compressed flexible duct compared with that of the sheet metal elbows.

TABLE 8. Results of the Bent Flexible Duct Tests

Section Diameter in (mm)	Bending Angle θ °	Compression Ratio r_c	Section Length L in (mm)	Radius-to-Diameter Ratio r/D	Local Loss Coefficient K
6 (150 mm)	90	0.05	19 (480)	2.50	1.18
		0.186	50 (1270)	5.00	3.27
	45	0.048	46 (1170)	9.67	1.76
		0.243	36 (915)	4.00	3.13
	135	0.048	30 (760)	1.83	1.90
		0.305	24 (610)	1.67	3.12
8 (200 mm)	90	0.136	36 (915)	2.00	2.85
		0.342	35 (890)	2.50	2.31
	45	0.118	34 (85)	2.75	2.26
		0.305	22 (560)	2.38	1.85
	135	0.077	36 (915)	2.38	2.84
		0.331	32 (815)	2.00	2.54
10 (250 mm)	90	0.069	63 (1600)	4.20	1.73
		0.358	41 (1040)	2.70	1.35
	45	0.048	54 (1370)	6.80	1.15
		0.336	24 (610)	3.80	0.87
	135	0.050	69 (1750)	2.20	1.55
		0.338	39 (990)	1.40	1.45

Splitter Box Tests

Three sizes of duct board splitter boxes were tested, 10”x8”x6” (250x200x150 mm), 10”x8”x8” (250x200x200 mm), and 8”x6”x6” (200x150x150 mm). The three numbers refer to the inlet diameter and the two outlet diameters respectively. The tests were performed for each splitter box before and after sealing with mastic. Splitter 10”x8”x6” leaked 2.6 cfm@25Pa (1.2 L/s@25Pa) before sealing, and 0.4 cfm@25Pa (0.2 L/s@25Pa) after sealing. Splitter 10”x8”x8” leaked 2.6 cfm@25Pa (1.2 L/s@25Pa) before sealing, and 0.6 cfm@25Pa (0.3 L/s@25Pa) after sealing. Splitter 8”x6”x6” leaked 2.8 cfm@25Pa (1.3 L/s@25Pa) before sealing, and 0.5 cfm@25Pa (0.2 L/s@25Pa) after sealing. Figure 14 illustrates how these leakage tests were performed. Two of the three openings were capped and sealed. A small fan was connected to the third opening to pressurize the splitter box to 25 Pa. The air flow rate required to reach this pressure was determined by a small nozzle flow meter in line with the fan.

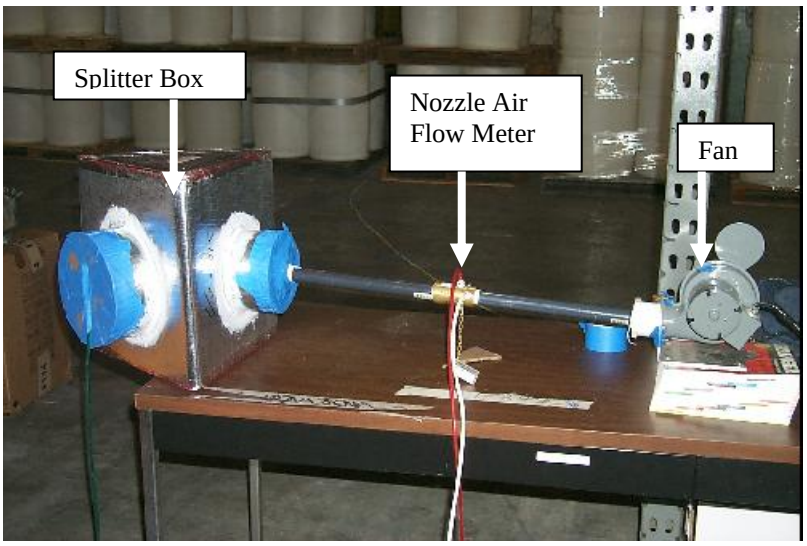

Figure 14. *Leakage test on a 10”x8”x6” (250x200x150 mm) sealed splitter box.*

The pressure drops and loss coefficients were determined separately for each splitter box branch. This required a piezometer be placed on each individual branch together with fans to control the amount of flow in each branch. These two fans are also used as flow measuring devices. A nozzle flowmeter was attached to the main leg of the splitter box, and acted as a check on the total flow from the two branches. The following equations were used to determine the local loss coefficient of each branch of the splitter boxes. These relationships account for the pressure drop in the straight sections of duct upstream and downstream of the splitter box so as to obtain results for the splitter box only.

$$\text{IP:}\quad \Delta P_{X-Y} = \Delta P_{1-2} - \left(L_1\right)\left(c_1 Q_1^{n_1}\right) + \rho\left(\left(\frac{V_1}{1097}\right)^2 - \left(\frac{V_2}{1097}\right)^2\right) - \left(L_2\right)\left(c_2 Q_2^{n_2}\right)$$

$$\text{SI:}\quad \Delta P_{X-Y} = \Delta P_{1-2} - \left(L_1\right)\left(c_1 Q_1^{n_1}\right) + \rho\left(\frac{(V_1)^2}{2} - \frac{(V_2)^2}{2}\right) - \left(L_2\right)\left(c_2 Q_2^{n_2}\right) \qquad (17)$$

and,

$$\text{IP:}\quad \Delta P_{X-Z} = \Delta P_{1-3} - \left(L_1\right)\left(c_1 Q_1^{n_1}\right) + \rho\left(\left(\frac{V_1}{1097}\right)^2 - \left(\frac{V_3}{1097}\right)^2\right) - \left(L_3\right)\left(c_3 Q_3^{n_3}\right)$$

$$\text{SI:}\quad \Delta P_{X-Z} = \Delta P_{1-3} - \left(L_1\right)\left(c_1 Q_1^{n_1}\right) + \rho\left(\frac{\left(V_1\right)^2}{2} - \frac{\left(V_3\right)^2}{2}\right) - \left(L_3\right)\left(c_3 Q_3^{n_3}\right) \qquad (18)$$

where:

ΔP_{X-Z} and ΔP_{X-Y} = Total pressure drop along the specific branch path of the splitter box
ΔP_{1-2} and ΔP_{1-3} = Total pressure drop from upstream (main) to downstream (branch) piezometers
L_1, L_2 and L_3 = Upstream (main) and downstream (branch) lengths of the sheet metal duct sections
c_1, c_2 ,*and* c_3 =Power law pressure coefficients of the upstream (main) and downstream (branch) sheet metal ducts (different sizes)
Q_1, Q_2 and Q_3 = Upstream (main) and downstream (branch) volumetric flow rate
n_1, n_2 ,*and* n_3 = Volumetric flow rate power law exponents of the upstream (main) and downstream (branch) sheet metal ducts (different sizes)
ρ = air density
V_1, V_2 and V_3 = Upstream (main) and downstream (branch) velocities

After calculating the total pressure drop along a specific branch path of the splitter box, the loss coefficients were calculated as follows.

$$\text{IP:}\quad K_{X,Y} = \frac{\Delta P_{X-Y}}{\rho\left(\frac{V_Y}{1097}\right)^2}$$

$$\text{SI:}\quad K_{X,Y} = \frac{\Delta P_{X-Y}}{\rho\frac{\left(V_Y\right)^2}{2}} \qquad (19)$$

and,

$$\text{IP:}\quad K_{X,Z} = \frac{\Delta P_{X-Z}}{\rho\left(\frac{V_Z}{1097}\right)^2}$$

$$\text{SI:}\quad K_{X,Z} = \frac{\Delta P_{X-Z}}{\rho\frac{\left(V_Z\right)^2}{2}} \qquad (20)$$

The standard method of reporting local loss coefficients for diverging and converging junctions is the flow rate ratio (branch-to-main) and the corresponding loss coefficient through that branch. Pressure/flow stations were uniformly designed so that the flow rate ratio changed in approximately equal steps between *0* and *1*. For the symmetrical splitter boxes (10”x8”x8” and 8”x6”x6”) the calculated loss coefficients for the identical branches were not exactly equal. This was caused by the uncertainty of maintaining identical branch-to-main flow ratios, between the

two branches, at each pressure/flow station. The reported loss coefficients for these symmetrical and splitter boxes were therefore the averages of the symmetrical branches values (sealed splitter box only). Figure 15 shows a splitter box test specimen. Tables 9, 10 and 11 include the results of the six tests performed on the three sizes of splitter boxes.

Figure 15. *10"x8"x8" (250x200x200 mm) Splitter Box test apparatus including two duct blasters (on the branches) and a nozzle flowmeter on the main.*

TABLE 9. The 10"x8"x6" (250x200x200 mm) Splitter Box Local Loss Coefficients

D_1 = 10" (250 mm), D_2 = 6" (150 mm), D_3 = 8" (200 mm)								
As-is	Q_3/Q_1	0.00	0.18	0.33	0.49	0.67	0.82	1.00
	$K_{1,3}$	**-**	**7.23**	**2.74**	**2.16**	**1.54**	**1.20**	**0.89**
	Q_2/Q_1	1.00	0.82	0.67	0.51	0.33	0.18	0.00
	$K_{1,2}$	**0.62**	**0.71**	**0.82**	**0.78**	**0.96**	**1.59**	**-**
Sealed	Q_3/Q_1	0.00	0.18	0.33	0.49	0.67	0.82	1.00
	$K_{1,3}$	**-**	**6.34**	**2.58**	**1.94**	**1.48**	**1.15**	**0.87**
	Q_2/Q_1	1.00	0.82	0.67	0.51	0.33	0.18	0.00
	$K_{1,2}$	**0.63**	**0.68**	**0.82**	**0.88**	**1.03**	**1.91**	**-**

TABLE 10. The 10"x8"x8" (250x200x200 mm) Splitter Box Local Loss Coefficients

D_1 = 10" (250 mm), D_2 = 8" (200 mm), D_3 = 8" (200 mm)						
As-is	Q_3/Q_1	1.00	0.73	0.49	0.26	0.00
	$K_{1,3}$	**0.81**	**0.99**	**1.67**	**4.09**	**-**
	Q_2/Q_1	0.00	0.27	0.51	0.74	1.00
	$K_{1,2}$	**-**	**4.08**	**1.36**	**0.79**	**0.52**
Sealed	Q_3/Q_1	1.00	0.73	0.50	0.27	0.00
	$K_{1,3}$	**0.75**	**0.94**	**1.61**	**4.07**	**-**
	Q_2/Q_1	0.00	0.27	0.50	0.73	1.00
	$K_{1,2}$	**-**	**3.94**	**1.30**	**0.76**	**0.52**
	Q_b/Q_m	0.00	0.27	0.50	0.73	1.00
	$K_{m\text{-}b,\ average}$	**-**	**4.00**	**1.45**	**0.85**	**0.63**

TABLE 11. The 8”x6”x6” (200x150x150 mm) Splitter Box Local Loss Coefficients

D_1 = 8” (200 mm), D_2 = 6” (150 mm), D_3 = 6” (150 mm)						
As-is	Q_3/Q_1	1.00	0.73	0.50	0.27	0.00
	$K_{1,3}$	**0.84**	**0.70**	**1.08**	**2.84**	**-**
	Q_2/Q_1	0.00	0.27	0.50	0.73	1.00
	$K_{1,2}$	**-**	**3.22**	**1.25**	**0.73**	**0.84**
Sealed	Q_3/Q_1	1.00	0.73	0.50	0.27	0.00
	$K_{1,3}$	**0.51**	**0.70**	**1.21**	**3.39**	**-**
	Q_2/Q_1	0.00	0.27	0.50	0.73	1.00
	$K_{1,2}$	**-**	**2.77**	**1.02**	**0.72**	**0.71**
	Q_b/Q_m	0.00	0.27	0.50	0.73	1.00
	$K_{m\text{-}b,\ average}$	**-**	**3.08**	**1.11**	**0.71**	**0.61**

The results showed that the local loss coefficient through a branch of the splitter box could vary between 0.6 and 6.3 depending on geometry and flow ratios. A typical result is 1.0 and 1.5 for the smaller and the larger branch of a 10”x8”x6” (250x200x150 mm) splitter box, respectively, when the flow is balanced. ASHRAE Fundamentals shows local loss coefficients values for rectangular “Tee’s” and “Wye’s” that cover the range of the results obtained in this study. However, ASHRAE Fundamentals does not show data for splitter boxes. ACCA Manual D provides pressure drop for splitter boxes, in terms of equivalent length (EL), independent of size. For an air velocity of 700 fpm (3.6 m/s) (typical maximum value for a residential air distribution system), ACCA’s splitter box EL value corresponds to a static pressure value of 0.08 in water (19.9 Pa), compared with a total pressure value of 0.045 in water (11.2 Pa) based on our calculated loss coefficients (for the larger branch of the 10”x8”x6” splitter box, assuming a 0.67 flow rate ratio). The values in ACCA Manual D, therefore, overestimate the pressure drop in splitter boxes compared to our test results.

Kokayko et al. (1996) provided static pressure data for splitter boxes with symmetrical outlets. A single value for the static pressure drop across the splitter box is reported. It is not clear whether the values reported can be used for a single branch of the splitter, or as a total for both. The authors indicated that they took a pressure reading inside the box for their calculations. Pressure inside in the box are very unstable due to turbulance and separation and very hard to read. The correct way to measure the pressure drop is at enough distances upstream and downstream of the splitter box, as indicated in ASHRAE (1995). Therefore, we did not attempt to compare our splitter box results with the mentioned document.

Supply Boots

Three types of supply boots were tested: 8” (200 mm) diameter neck Angle Supply, 8” (200 mm) Straight Supply, and 6” (150 mm) Straight Supply. Each boot was mounted on a plywood sheet wall, and tested with and without diffuser. Because the straight supply boots are unlikely to be supplied by a straight flexible duct in a typical installation, they were tested with a 90° flexible duct elbow. Two geometries were tested for the added flexible duct: *Angle 1* is when the boot is fed from the duct along the axis of its narrow dimension, and *Angle 2* is when the boot is fed from the duct along the axis of its wide dimension. All supply boots were tested following the requirements of “Duct-mounted Exit Fitting” from ASHRAE Standard 120P. Figure 16 shows the various configurations of the supply boots tests.

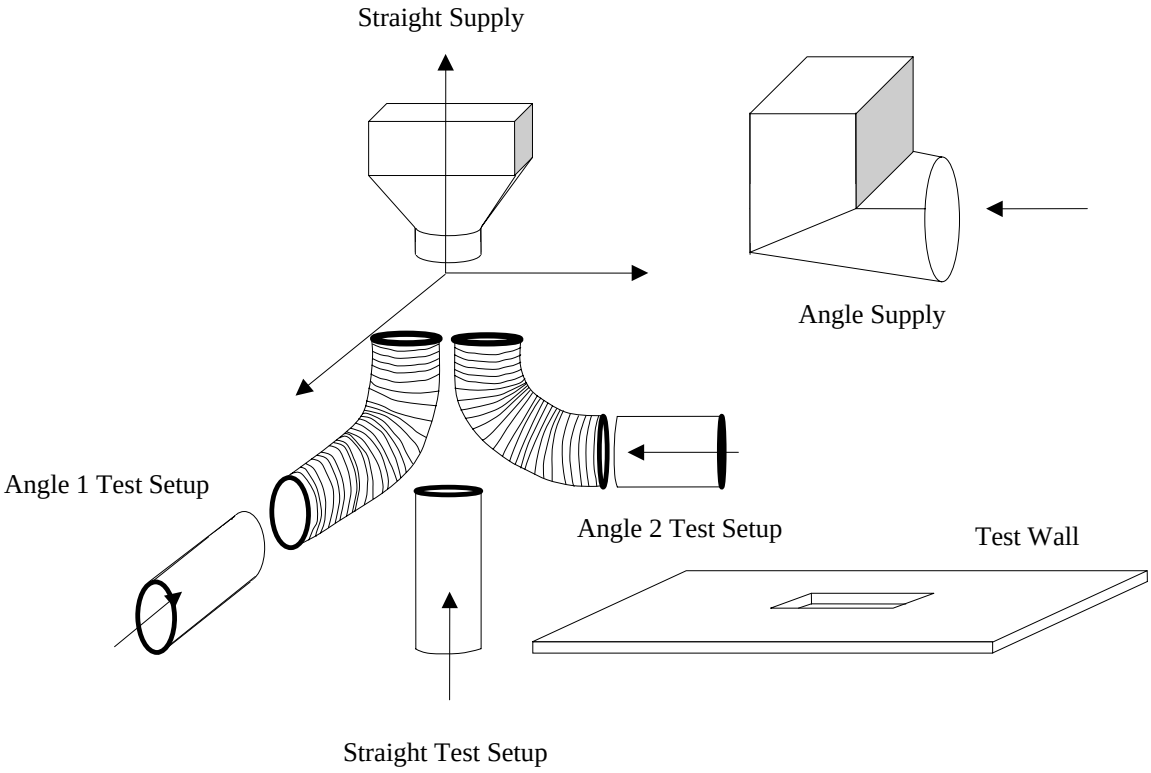

Figure 16. *Different configurations of connecting the supply boots to the supply duct as used in the tests, including the attachment to a wall, with and without diffuser.*

The local loss coefficients for the supply boot were corrected for the pressure drop in the associated pressure measuring sections using:

$$\text{IP:}\quad \Delta P_T = P_1 + \rho\left(\frac{V_1}{1097}\right)^2 - \left(L_1\right)\left(c_1 Q_1^{n_1}\right)$$

$$\text{SI:}\quad \Delta P_T = P_1 + \rho\frac{\left(V_1\right)^2}{2} - \left(L_1\right)\left(c_1 Q_1^{n_1}\right) \qquad (21)$$

where:

ΔP_T = Total pressure drop in the supply boot
P_1 = Static pressure at the piezometer, upstream of the supply boot
ρ = Air density
V_1 = Upstream air velocity in the sheet metal duct serving the supply boot
L_1 = Length of the sheet metal duct serving the supply boot
c_1 = Power law pressure coefficient of the upstream sheet metal duct
Q_1 = Volumetric flow rate
n_1 = Volumetric flow rate power law exponent sheet metal duct

After calculating the total pressure drop in the supply boot, the local loss coefficient is calculated as follows.

$$\text{IP:}\quad K = \frac{\Delta P_T}{\rho\left(\frac{V_1}{1097}\right)^2}$$

$$\text{SI:}\quad K = \frac{\Delta P_T}{\frac{\rho}{2}V_1^2} \tag{22}$$

Tables 12, 13 and 14 show the results of the supply boots tests.

TABLE 12. Local Loss Coefficients of Various Configurations of the 8" (200 mm) Neck Diameter Angle Supply Boot

Type	Angle Supply Boot	
Setup	With Diffuser	Without Diffuser
K	2.43	1.23
Boot Neck Diameter in (mm)	8 (200)	8 (200)

TABLE 13. Local Loss Coefficients of Various Configurations of the 8" (200 mm) Neck Diameter Straight Supply Boot

	Type	Straight Supply Boot					
	Setup	Angle 1		Angle 2		Straight	
		With Diffuser	Without Diffuser	With Diffuser	Without Diffuser	With Diffuser	Without Diffuser
	K	3.86	3.03	3.77	2.87	1.76	1.02
	Boot Neck Diameter in (mm)	8 (200)	8 (200)	8 (200)	8 (200)	8 (200)	8 (200
Flexible Duct Section	**Length in (mm)**	19 (480)	19 (480)	19 (480)	19 (480)	-	-
	Radius in (mm)	13 (330)	13 (330)	13 (330)	13 (330)	-	-
	Compression Ratio r_c	0.457	0.457	0.457	0.457	-	-

TABLE 14. Local Loss Coefficients of Various Configurations of the 6" (150 mm) Neck Diameter Straight Supply Boot

	Type	Straight Supply Boot					
	Setup	Angle 1		Angle 2		Straight	
		With Diffuser	Without Diffuser	With Diffuser	Without Diffuser	With Diffuser	Without Diffuser
	K	5.31	4.61	4.57	4.28	1.30	0.98
	Boot Neck Diameter in (mm)	6 (150)	6 (150)	6 (150)	6 (150)	6 (150)	6 (150)
Flexible Duct Section	**Length in (mm)**	21 (530)	21 (530)	21 (530)	21 (530)	-	-
	Radius in (mm)	14 (355)	14 (355)	14 (355)	14 (355)	-	-
	Compression Ratio r_c	0.19	0.19	0.19	0.19	-	-

The supply boots results showed that diffusers have a major effect on the pressure losses in exit fittings. The diffuser increases the loss coefficient by factors between 1.1 and 2.0, depending on the configuration of the boot connection. ASHRAE Fundamentals does not provide pressure loss data for air supply boots as they are found in typical installations. For added flex duct cases, the pressure drop increased by factors between 3 and 4, compared with the figures obtained when the boot is connected to a straight sheet metal duct. ACCA Manual D provides equivalent length values for the supply boots, and includes a value for a supply boot having a flexible elbow attached to it. Our test results show that ACCA Manual D values underestimate the pressure drop in the boots. For instance for an 8" (200 mm) Straight Supply Boot – Angle 1 with Diffuser, at an air velocity of 900 fpm (4.5 m/s) (reference value for ACCA values) our calculated loss coefficient provides a total pressure drop of 0.19 in water (47 Pa) (0.14 in water (35 Pa), static), while ACCA EL values corresponds to 0.02 in water (5 Pa) of static pressure.

Air-Intake Hood

The hood was mounted on a wooden wall, and tested as required by ASHRAE Standard 120P for "Duct-mounted Entry Fitting". Figure 17 shows the air intake hood test setup. The local loss coefficient of the intake hood was *4.1*; a substantial factor in the pressure drop to be considered when designing the ducting system. A similar hood could not be found in the literature for a comparison. ASHRAE Fundamentals indicates in Table CD6-1, page 34.31, that a screen (only), having the exact size of the ducted inlet has a loss coefficient between 0.0 and 6.2, depending on the free area ratio of the screen. ASHRAE Fundamentals 2001 gives a loss coefficient value of 0.5 (duct flush with wall) for a "Duct Mounted in Wall" in table ED1-1, page 34.32. ACCA Manual D does not include outside air-intake hoods.

Figure 17. *The air intake hood test setup.*

COMPLETE AIR DISTRIBUTION SYSTEM ANALYSIS

The second part of the study applied the individual component analyses to a complete duct system to check that the individual components can be combined to produce the same system pressures as a fully assembled complete system. A complete full-scale residential air distribution system was built in the Energy Performance of Buildings Group Duct Lab. This duct system was designed to be representative of duct systems found in California houses and is based on a survey of 20 homes. The system had 11 supply registers and a single return, with a total system flow of 1,200 cfm (566 L/s) and its layout and other details are shown in Figure 18. All duct runs were as straight as possible and the ducts were cut to the correct length so as not to compress the ducts. The average compression ratio in all the flexible duct runs was 10%. The ducts are hung below a plywood deck, with the register boots attached to the underside of the deck. The system was carefully sealed and its leakage measured using a pressurization test was only 9 cfm (4 L/s) at 25 Pa.

The air flow was measured at every register using a powered flow hood. The total system air flow was measured using a high-precision (±0.5%) flow nozzle between the return grille and the air handler fan. In addition pressures were measured in several locations throughout the system including the supply and return plenums. These flow measurements, together with the power law pressure drop models and the local loss coefficients developed in the component analysis were used to calculate the pressure drop in the supply branches of the system. The calculated pressure drop in the supply branches were then compared to the measured static pressure in the supply plenum. These measured system static pressures were also compared to existing ASHRAE and ACCA data and calculation methods.

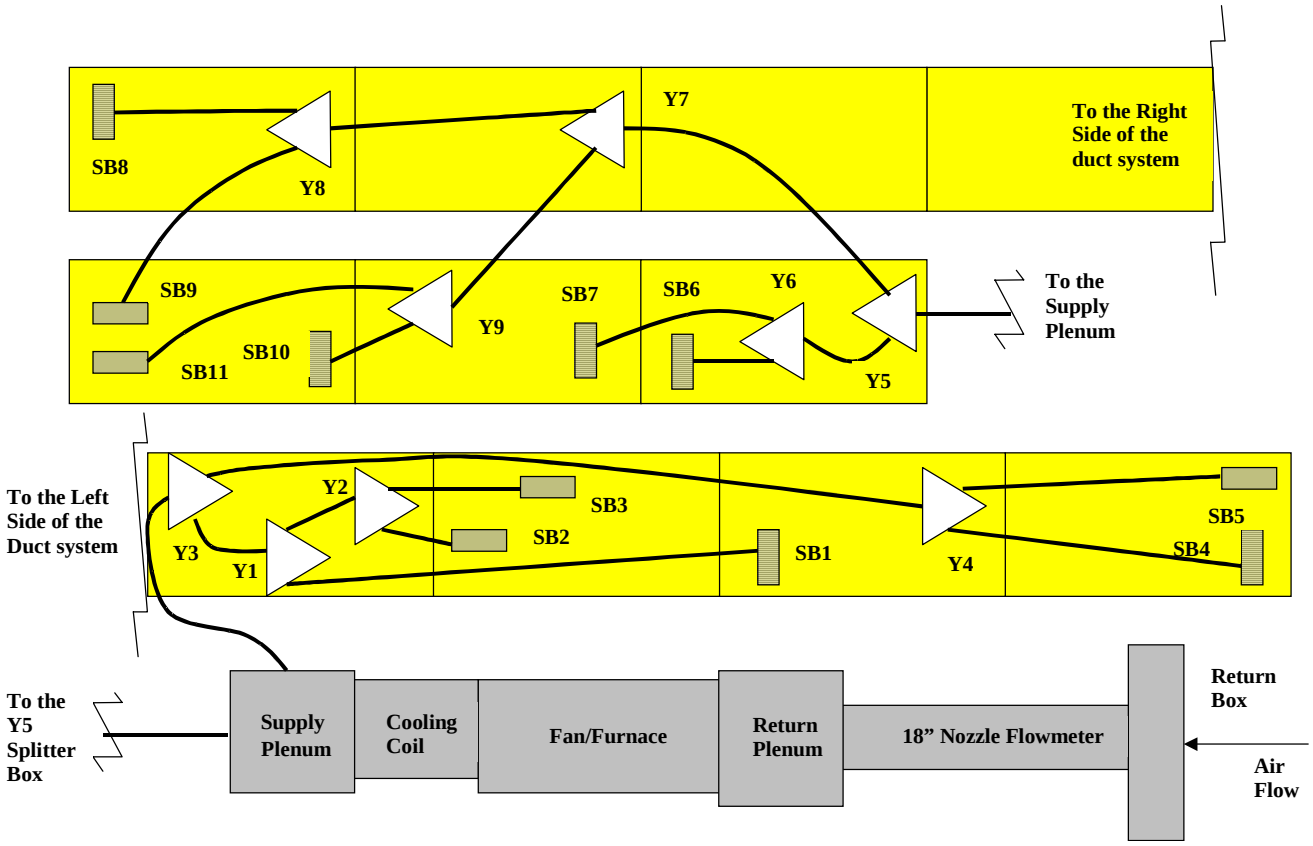

Figure 18. *A schematic of the air distribution system installed at the EPB Duct Lab.*

The supply side of the air distribution system was divided into different sections at all points where flow, size, or shape changes. The total pressure drop for each section was calculated by adding the static pressure drop in the flexible duct part of the section (based on the power law models and the pressure drop correction factors developed in the component analysis) to the total pressure drops in the fittings. Tables A1 through A6 in the Appendix show the local loss coefficient summary by sections of the supply side of the installed system. The results of all these calculations are summarized in Table 15. The calculations based on the individual component measurements performed for this study gave the closest results to the measured static pressure in the supply plenum. ACCA Manual D underpredicts the pressure drop in the flexible duct and the supply boots while it overpredicts the pressure drop in the splitter boxes, resulting in an overprediction of the pressure drop in the supply plenum. ASHRAE Fundamentals 2001 underpredicts the pressure drop in both the flexible duct and the rest of the duct fittings, resulting in an underprediction of the static pressure in the supply plenum.

TABLE 15. Comparison of the Installed System Calculations as Compared with Measured Static Pressure in the Supply Plenum

	Calculated Static Pressure at Entry in water (Pa)		Measured Static Pressure in the Upper Four Corners of the Supply Plenum in water (Pa)
	Branch SP-Y5	Branch SP-Y3	
Component Analysis	0.168 (41.8)	0.122 (30.4)	0.168, 0.130, 0.130, and 0.156 (41.8, 32.4, 32.4, and 38.8)
ACCA Manual D	0.191 (47.6)	0.122 (30.4)	
ASHRAE Fundamentals 2001	0.123 (30.6)	0.085 (21.2)	

The differences between the measured and predicted pressures are due to violating the criteria followed in the testing of the individual components where the flows are fully developed and undisturbed upstream and downstream of each component, and uncertainty in the measured plenum static pressures. Thus in an actual installation, the flow pattern, in terms of velocity and pressure profiles of the air circulating in different components of the system is different from that of the air passing through every single component when tested individually. Moreover, there are extrapolation errors for duct sizes not covered in the components analysis (diameters greater than 10" (250 mm) for flexible duct and splitter boxes). Lastly, the uncertainty in the measured static pressures is because this pressure changes with location within the plenum and there is no single value to compare with the calculated pressures.

SUMMARY

This paper describes the tests performed and summarizes the results that help as new data for residential duct design. The paper covers the description and the results of the individual tests on the duct components, and the analysis of the whole ducting system, as installed. The results on the tested air distribution system components were used in the complete duct system analysis and compared with available data from the literature. The comparison showed that our new data provide a better estimation of the total pressure drop. The paper also includes a detailed study of the compression effects on pressure losses in flexible ducts, and proposes a new semiempirical model to calculate the pressure drop in flexible ducts. Major findings from the work are summarized below:

- The work showed that the ASHRAE Standard 120 test procedure should be revised to require a tight connection of the inner liner only, of the test specimen, with enough duct tape to the rigid duct, without clamping the outer layers (insulation and outer plastic sheet).
- The results of compressed ducts also showed that when a flexible duct is compressed, it can have a greater pressure drop per unit length than a fully stretched duct of a smaller diameter.
- The prediction of the pressure drops using the modeled friction factors were within 0.5% (on average) of the measured values, with all results within 9%.
- The flexible duct elbows have much higher local loss coefficients than those reported for sheet metal elbows, and ranging between 0.9 and 3.3 for the duct sizes tested. These higher values can be explained by the increased absolute surface roughness of the compressed flexible duct compared with that of the sheet metal elbows.
- The local loss coefficient through a branch of the splitter box could vary between 0.6 and 6.3 depending on geometry and flow ratios.

- The supply boots results showed that diffusers have a major effect on the pressure losses in exit fittings. The diffuser increases the loss coefficient by factors between 1.1 and 2.0, depending on the configuration of the boot connection. For added flex duct cases, the pressure drop increased by factors between 3 and 4, compared with the figures obtained when the boot is connected to a straight sheet metal duct.

ACKNOWLEDGEMENTS

This work at the Lawrence Berkeley National Laboratory was funded by Pacific Gas and Electric Company under Contract S9902A, to support PG&E's energy efficiency programs in new and existing residential buildings via the California Institute for Energy Efficiency under Contract No. S9902A. Publication of research results does not imply CIEE endorsement of or agreement with these findings, nor that of any CIEE sponsor.

This work was also supported by the Assistant Secretary for Energy Efficiency and Renewable Energy, Office of Building Technology, State and Community Programs, Office of Building Research and Standards, of the U.S. Department of Energy under Contract No. DE-AC03-76SF00098.

NOMENCLATURE

a = slope of the linear equation of the pressure drop correction factor, dimensionless
C = pressure drop coefficient (in water/100ft cfm^n), (Pa s^n/m.L^n)
D = flexible duct diameter (in), (mm)
ε = absolute surface roughness of the duct (ft), (mm)
f, f' = friction factor, dimensionless
K = local loss coefficient, dimensionless
L = duct length (ft) (m)
n = volumetric flow rate exponent
N = number of data point measured in a test
$PDCF$ = pressure drop correction factor
Q = volumetric flow rate (cfm), (L/s)
r_c = compression ratio, dimensionless
Re = Reynolds Number, dimensionless
V = air velocity (fpm), (m/s)
T = air temperature (°F), (°C)

Greek Symbols

ΔP = pressure drop per unit length (in water/100 ft), (Pa/m)
ΔP_f = pressure drop (in water), (Pa)
λ = pitch of the flexible duct (distance between two consecutive wire spirals) (in), (mm)
ρ = air density (lbm/ft^3), (kg/m^3)

Subscripts

FS = fully stretched
Norm = normalized

REFERENCES

ACCA. 1995. *Residential Duct Systems. Manual D.* Air Conditioning Contractors of America. Washington, DC.

ASHRAE. 2001. ASHRAE *Handbook of Fundamentals*. American Society of Heating Refrigerating and Air-conditioning Engineers, Atlanta, Georgia.

ASHRAE. 1995. *ASHRAE Standard 120P, Methods of Testing to Determine Flow Resistance of HVAC Air Ducts and Fittings, December 1995*. American Society of Heating Refrigerating and Air-conditioning Engineers, Atlanta, Georgia.

ASTM E779. 1999. *Standard Test Method for Determining Air Leakage Rate by Fan Pressurization*. American Society of Testing and Materials. West Conshohocken, PA.

Altshul, A.D. and P.G. Kiselev. 1975. *Hydraulics and Aerodynamics*. Stroisdat Publishing House, Moscow, USSR.

Energy Conservatory. 1996. *Minneapolis Duct Blaster (Series B) Operation Manual*. The Energy Conservatory. Minneapolis, MN.

IBACOS 1995. *Ventilation Ducts and Registers – Interim Milestone Report*. IBACOS, Pittsburgh, PA.

Kokayko, M., Holton, J., Beggs, T., Walthour, S., and Dickson, B. 1996. *Residential Ductwork and Plenum Box Bench Tests*. IBACOS – Burt Hill Project 95006.13. Pittsburgh, PA.

Tsal, R.J. 1989. Altshul-Tsal friction factor equation. *Heating, Piping and Air Conditioning* (August).

Appendix. Results of the Complete Air Distribution System Analysis

TABLE A1. Local Loss Coefficient Summary By Sections of the Supply Side of the Installed System Based on the Component Analysis

Duct Section	Installed Fitting	Type of Fitting From Component Analysis	Parameters	Local Loss Coefficient[c]
SP-Y5	Collar Entry	Bellmouth, Plenum to Round[b]	r/D = 0	***0.5***
Y5-Y6	Splitter Box Y5 14"x12"x10"[a] (356x305x250 mm)	Splitter Box 14"x12"x10" Branch 10" (250 mm)	Q_2/Q_1 = 0.39	***2.24***
Y5-Y7	Splitter Box Y5 14"x12"x10"[a] (356x305x250 mm)	Splitter Box 14"x12"x10" Branch 12" (305 mm)	Q_3/Q_1 = 0.61	***1.97***
Y6-SB6	Splitter Box Y6 10"x8"x6" (250x200x150 mm)	Splitter Box 10"x8"x6" Branch 8" (200 mm)	Q_3/Q_1 = 0.71	1.45
	Supply Boot SB6	8" (200 mm) Straight Supply Boot (Angle 1, with Diffuser)		3.86
	Total Loss Coefficients			***5.31***
Y6-SB7	Splitter Box Y6 10"x8"x6" (250x200x150 mm)	Splitter Box 10"x8"x6" Branch 6" (150 mm)	Q_2/Q_1 = 0.29	1.13
	Supply Boot SB7	6" (150 mm) Straight Supply Boot (Angle 1, with Diffuser)		5.31
	Total Loss Coefficients			***6.44***
Y7-Y9	Splitter Box Y7 12"x10"x10"[d] (305x250x250 mm)	Splitter Box 12"x10"x10" Branch 10" (250 mm)	Q_2/Q_1 = 0.46	***2.46***
Y7-Y8	Splitter Box Y7 12"x10"x10"[d] (305x250x250 mm)	Splitter Box 12"x10"x10" Branch 10" (250 mm)	Q_2/Q_1 = 0.54	***1.74***
Y9-SB10	Splitter Box Y9 10"x8"x6" (250x200x150 mm)	Splitter Box 10"x8"x6" Branch 8" (200 mm)	Q_3/Q_1 = 0.63	1.68
	Supply Boot SB10	8" (200 mm) Angle Supply Boot (with Diffuser)		2.43
	Total Loss Coefficients			***4.11***
Y9-SB11	Splitter Box Y9 10"x8"x6" (250x200x150 mm)	Splitter Box 10"x8"x6" Branch 6" (150 mm)	Q_2/Q_1 = 0.37	0.92
	Supply Boot SB11	6" (150 mm) Straight Supply Boot (Angle 2, with Diffuser)		4.57
	Total Loss Coefficients			***5.49***
Y8-SB8	Splitter Box Y8 (10"x8"x6") (250x200x150 mm)	Splitter Box 10"x8"x6" Branch 8" (200 mm)	Q_3/Q_1 = 0.63	1.68
	Supply Boot SB8	8" (200 mm) Straight Supply Boot (Angle 2, with Diffuser)		3.77
	Total Loss Coefficients			***5.45***
Y8-SB9	Splitter Box Y8 10"x8"x6" (250x200x150 mm)	Splitter Box 10"x8"x6" Branch 6" (150 mm)	Q_2/Q_1 = 0.37	0.92
	Supply Boot SB9	6" (150 mm) Straight Supply Boot (Angle 2, with Diffuser)		4.57
	Total Loss Coefficients			***5.49***
SP-Y3	Collar Entry	Bellmouth, Plenum to Round[b]	r/D = 0	***0.5***
Y3-Y1	Splitter Box Y3 12"x10"x10"[d] (305x250x250 mm)	Splitter Box 12"x10"x10" Branch 10" (250 mm)	Q_2/Q_1 = 0.53	***1.78***
Y3-Y4	Splitter Box Y3 12"x10"x10"[d] (305x250x250 mm)	Splitter Box 12"x10"x10" Branch 10" (250 mm)	Q_2/Q_1 = 0.47	***2.32***
Y1-SB1	Splitter Box Y1 10"x8"x8" (250x200x200 mm)	Splitter Box 10"x8"x8" Branch 8" (200 mm)	Q_2/Q_1 = 0.57	1.27
	Supply Boot SB1	8" (200 mm) Straight Supply Boot (Angle 1, with Diffuser)		3.86
	Total Loss Coefficients			***5.13***

TABLE A1. Local Loss Coefficient Summary By Sections of the Supply Side of the Installed System Based on the Component Analysis (Continued)

Duct Section	Installed Fitting	Type of Fitting From Component Analysis	Parameters	Local Loss Coefficient[c]
Y1-Y2	Splitter Box Y1 10”x8”x8” (250x200x200 mm)	Splitter Box 10”x8”x8” Branch 8” (200 mm)	$Q_2/Q_1 = 0.43$	***2.23***
Y2-SB2	Splitter Box Y2 8”x6”x6” (200x150x150 mm)	Splitter Box 8”x6”x6” Branch 6” (150 mm)	$Q_2/Q_1 = 0.59$	0.95
	Supply Boot SB2	6” (150 mm) Straight Supply Boot (Angle 2, with Diffuser)		4.57
	Total Loss Coefficients			***5.52***
Y2-SB3	Splitter Box Y2 8”x6”x6” (200x150x150 mm)	Splitter Box 8”x6”x6” Branch 6” (150 mm)	$Q_2/Q_1 = 0.41$	1.88
	Supply Boot SB3	6” (150 mm) Straight Supply Boot (Angle 2, with Diffuser)		4.57
	Total Loss Coefficients			***6.45***
Y4-SB4	Splitter Box Y4 10”x8”x6” (250x200x150 mm)	Splitter Box 10”x8”x6” Branch 8” (200 mm)	$Q_3/Q_1 = 0.62$	1.71
	Supply Boot SB4	8” (200 mm) Straight Supply Boot (Angle 2, with Diffuser)		3.77
	Total Loss Coefficients			***5.48***
Y4-SB5	Splitter Box Y4 10”x8”x6” (250x200x150 mm)	Splitter Box 10”x8”x6” Branch 6” (150 mm)	$Q_2/Q_1 = 0.38$	0.91
	Supply Boot SB5	6” (150 mm) Straight Supply Boot (Angle 2, with Diffuser)		4.57
	Total Loss Coefficients			***5.48***

[a]Values are estimated based on ASHRAE Fundamentals 2001 (IP), Table SR5-11, page 34.65.
[b]ASHRAE Fundamentals 2001 (IP), Table SD1-1, page 34.48.
[c]Loss coefficient values of the splitter boxes are interpolated from the components analysis results to correspond to the exact flow rate ratios.
[d]Values are estimated (extrapolation based on smaller sizes of tested splitter boxes).

TABLE A2. Total Pressure Calculations By Sections of the Supply Side of the Installed System Based on the Component Analysis

Duct Section	Duct Element	Flow Rate[a] cfm (L/s)	Duct Size in (mm)	Velocity fpm (m/s)	Velocity Pressure in water (Pa)	Fully Stretched Duct Length ft (m)	Installed Duct Length ft (m)	Compression Ratio r_c	PDCF[b]	Net Installed Duct Length[c] ft (m)	Fitting Loss Coefficient C	Duct Pressure Drop[d] in water/100ft (Pa/m)	Total Pressure Drop in water (Pa)	Section Total Pressure Drop in water (Pa)
SP-Y5	Duct	757 (357.3)	14 (356)	708 (3.60)		2.67 (0.81)	2.17 (0.66)	0.19	3.24	2.17 (0.66)		0.182 (1.49)	0.004 (0.98)	
	Fitting	757 (357.3)		708 (3.60)	0.031 (7.76)						0.50		0.016 (3.88)	0.020 (4.86)
Y5–Y6	Duct	298 (140.7)	10 (250)	546 (2.78)		3.00 (0.91)	2.67 (0.81)	0.11	2.74	2.67 (0.81)		0.167 (1.37)	0.004 (1.11)	
	Fitting	298 (140.7)		546 (2.78)	0.019 (4.62)						2.24		0.042 (10.35)	0.046 (11.46)
Y5-Y7	Duct	459 (216.6)	12 (305)	584 (2.97)		12.00 (3.66)	12.00 (3.66)	0.00	1.00	12.00 (3.66)		0.055 (0.45)	0.007 (1.64)	
	Fitting	459 (216.6)		584 (2.97)	0.021 (5.28)						1.97		0.042 (10.41)	0.048 (12.05)
Y6-SB6	Duct	213 (100.5)	8 (200)	610 (3.10)		4.58 (1.40)	3.50 (1.07)	0.24	5.94	1.92 (0.59)		0.518 (4.23)	0.010 (2.48)	
	Fitting	213 (100.5)		610 (3.10)	0.023 (5.76)						5.31		0.123 (30.59)	0.133 (33.06)
Y6-SB7	Duct	85 (40.1)	6 (150)	433 (2.20)		11.00 (3.35)	9.17 (2.79)	0.17	5.47	7.46 (2.28)		0.430 (3.51)	0.032 (7.99)	
	Fitting	85 (40.1)		433 (2.20)	0.012 (2.90)						6.44		0.075 (18.67)	0.107 (26.66)
Y7-Y9	Duct	210 (99.1)	10 (250)	385 (1.96)		7.42 (2.26)	6.17 (1.88)	0.17	3.64	6.17 (1.88)		0.111 (0.90)	0.007 (1.70)	
	Fitting	210 (99.1)		385 (1.96)	0.009 (2.29)						2.46		0.023 (5.64)	0.029 (7.34)
Y7-Y8	Duct	249 (117.5)	10 (250)	457 (2.32)		9.58 (2.92)	8.67 (2.64)	0.10	2.50	8.67 (2.64)		0.107 (0.87)	0.009 (2.30)	
	Fitting	249 (117.5)		457 (2.32)	0.013 (3.22)						1.74		0.023 (5.61)	0.032 (7.91)

TABLE A2. Total Pressure Calculations By Sections of the Supply Side of the Installed System Based on the Component Analysis (Continued)

Duct Section	Duct Element	Flow Rate[a] cfm (L/s)	Duct Size in (mm)	Velocity fpm (m/s)	Velocity Pressure in water (Pa)	Fully Stretched Duct Length ft (m)	Installed Duct Length ft (m)	Compression Ratio r_c	PDCF[b]	Net Installed Duct Length[c] ft (m)	Fitting Loss Coefficient C	Duct Pressure Drop[d] in water/100ft (Pa/m)	Total Pressure Drop in water (Pa)	Section Total Pressure Drop in water (Pa)
Y9-SB10	Duct	132 (62.3)	8 (200)	378 (1.92)		6.00 (1.83)	5.50 (1.68)	0.08	2.74	3.92 (1.19)		0.096 (0.79)	0.004 (0.94)	
	Fitting	132 (62.3)		378 (1.92)	0.009 (2.21)						4.11		0.037 (9.09)	0.040 (10.03)
Y9-SB11	Duct	78 (36.8)	6 (150)	397 (2.02)		11.50 (3.51)	11.00 (3.35)	0.04	2.17	9.30 (2.83)		0.144 (1.17)	0.013 (3.32)	
	Fitting	78 (36.8)		397 (2.02)	0.010 (2.44)						5.49		0.054 (13.40)	0.067 (16.73)
Y8-SB8	Duct	156 (73.6)	8 (200)	447 (2.27)		6.50 (1.98)	5.42 (1.65)	0.17	4.48	3.84 (1.17)		0.216 (1.77)	0.008 (2.07)	
	Fitting	156 (73.6)		447 (2.27)	0.012 (3.09)						5.45		0.068 (16.84)	0.076 (18.91)
Y8-SB9	Duct	93 (43.9)	6 (150)	474 (2.41)		8.17 (2.49)	7.50 (2.29)	0.08	3.19	5.80 (1.77)		0.299 (2.45)	0.017 (4.32)	
	Fitting	93 (43.9)		474 (2.41)	0.014 (3.47)						5.49		0.076 (19.05)	0.094 (23.38)
SP-Y3	Duct	456 (215.2)	12 (305)	581 (2.95)		9.50 (2.90)	8.67 (2.64)	0.09	2.22	8.67 (2.64)		0.120 (0.98)	0.010 (2.59)	
	Fitting	456 (215.2)		581 (2.95)	0.021 (5.22)						0.50		0.010 (2.61)	0.021 (5.20)
Y3-Y1	Duct	242 (114.2)	10 (250)	444 (2.25)		2.28 (0.69)	2.17 (0.66)	0.05	1.78	2.17 (0.66)		0.072 (0.59)	0.002 (0.39)	
	Fitting	242 (114.2)		444 (2.25)	0.012 (3.05)						1.78		0.022 (5.42)	0.023 (5.81)
Y3-Y4	Duct	214 (101.0)	10 (250)	392 (1.99)		22.33 (6.81)	21.00 (6.40)	0.06	1.94	21.00 (6.40)		0.061 (0.50)	0.013 (3.19)	
	Fitting	214 (101.0)		392 (1.99)	0.010 (2.38)						2.32		0.022 (5.53)	0.035 (8.72)

TABLE A2. Total Pressure Calculations By Sections of the Supply Side of the Installed System Based on the Component Analysis (Concluded)

Duct Section	Duct Element	Flow Rate[a] cfm (L/s)	Duct Size in (mm)	Velocity fpm (m/s)	Velocity Pressure in water (Pa)	Fully Stretched Duct Length ft (m)	Installed Duct Length ft (m)	Compression Ratio r_c	PDCF[b]	Net Installed Duct Length[c] ft (m)	Fitting Loss Coefficient C	Duct Pressure Drop[d] in water/100ft (Pa/m)	Total Pressure Drop in water (Pa)	Section Total Pressure Drop in water (Pa)
Y1-SB1	Duct	139 (65.6)	8 (200)	398 (2.02)		19.67 (5.99)	19.00 (5.79)	0.03	1.71	17.42 (5.31)		0.066 (0.54)	0.012 (2.87)	
	Fitting	139 (65.6)		398 (2.02)	0.010 (2.45)						5.13		0.051 (12.58)	0.062 (15.46)
Y1-Y2	Duct	103 (48.6)	8 (200)	295 (1.50)		2.37 (0.72)	2.25 (0.69)	0.05	2.04	2.25 (0.69)		0.045 (0.37)	0.001 (0.25)	
	Fitting	103 (48.6)		295 (1.50)	0.005 (1.35)						2.23		0.012 (3.00)	0.013 (3.26)
Y2-SB2	Duct	61 (28.8)	6 (150)	311 (1.58)		5.75 (1.75)	5.00 (1.52)	0.13	4.50	3.30 (1.01)		0.183 (1.50)	0.006 (1.51)	
	Fitting	61 (28.8)		311 (1.58)	0.006 (1.49)						5.52		0.033 (8.24)	0.039 (9.75)
Y2-SB3	Duct	42 (19.8)	6 (150)	214 (1.09)		9.33 (2.84)	8.42 (2.57)	0.10	3.63	6.71 (2.05)		0.071 (0.58)	0.005 (1.18)	
	Fitting	42 (19.8)		214 (1.09)	0.003 (0.71)						6.45		0.018 (4.57)	0.023 (5.75)
Y4-SB4	Duct	132 (62.3)	8 (200)	378 (1.92)		12.33 (3.76)	11.00 (3.35)	0.11	3.26	9.42 (2.87)		0.115 (0.94)	0.011 (2.69)	
	Fitting	132 (62.3)		378 (1.92)	0.009 (2.21)						5.48		0.049 (12.12)	0.059 (14.81)
Y4-SB5	Duct	82 (38.7)	6 (150)	418 (2.12)		13.50 (4.11)	12.17 (3.71)	0.10	3.65	10.46 (3.19)		0.267 (2.18)	0.028 (6.96)	
	Fitting	82 (38.7)		418 (2.12)	0.011 (2.70)						5.48		0.059 (14.79)	0.087 (21.74)

[a]Measured flow values at each diffuser.
[b]Normalized pressure drop correction factor (It is estimated for sizes 12" (305 mm) and 14" (356 mm)).
[c]Net installed duct length is the total installed length minus the elbow that feeds the supply boot, as it is considered an integral part of the boot.
[d]Duct pressure drop is calculated by multiplying the pressure drop of the fully stretched duct by the corresponding PDCF (pressure drop for the 12" (305 mm) and 14" (356 mm) ducts is estimated by extrapolation from lower sizes).

TABLE A3. Equivalent Length Summary By Sections of the Supply Side of the Installed System Based on ACCA Manual D

Duct Section	Installed Fitting	ACCA Manual D Fitting Number	ACCA Manual D Type of Fitting[a, b]	Parameters	Effective Length[c]
SP-Y5	Collar Entry	Group 1 – A	Supply Air Fitting at the AHU		***35***
Y5-Y6	Splitter Box Y5 14”x12”x10” (356x305x250 mm)	Group 11	Junction Box	V = 546 fpm (L/s)	***62***
Y5-Y7	Splitter Box Y5 14”x12”x10” (356x305x250 mm)	Group 11	Junction Box	V = 584 fpm (L/s)	***71***
Y6-SB6	Splitter Box Y6 10”x8”x6” (250x200x150 mm)	Group 11	Junction Box	V = 610 fpm (L/s)	78
	Supply Boot SB6	Group 4 – AD	Supply Air Boot	V_{ref} = 900 fpm (L/s), V = 610 fpm (L/s)	28
	Total Loss Coefficients				***106***
Y6-SB7	Splitter Box Y6 10”x8”x6” (250x200x150 mm)	Group 11	Junction Box	V = 433 fpm (L/s)	40
	Supply Boot SB7	Group 4 – AD	Supply Air Boot	V_{ref} = 900 fpm (L/s), V = 433 fpm (L/s)	14
	Total Loss Coefficients				***54***
Y7-Y9	Splitter Box Y7 12”x10”x10” (305x250x250 mm)	Group 11	Junction Box	V = 385 fpm (L/s)	***33***
Y7-Y8	Splitter Box Y7 12”x10”x10” (305x250x250mm)	Group 11	Junction Box	V = 457 fpm (L/s)	***44***
Y9-SB10	Splitter Box Y9 10”x8”x6” (250x200x150 mm)	Group 11	Junction Box	V = 378 fpm (L/s)	32
	Supply Boot SB10	Group 4 – G	Supply Air Boot	V_{ref} = 900 fpm (L/s), V = 378 fpm (L/s)	14
	Total Loss Coefficients				***46***
Y9-SB11	Splitter Box Y9 10”x8”x6” (250x200x150 mm)	Group 11	Junction Box	V = 397 fpm (L/s)	35
	Supply Boot SB11	Group 4 – AD	Supply Air Boot	V_{ref} = 900 fpm (L/s), V = 397 fpm (L/s)	12
	Total Loss Coefficients				***47***
Y8-SB8	Splitter Box Y8 (10”x8”x6”) (250x200x150 mm)	Group 11	Junction Box	V = 447 fpm (L/s)	42
	Supply Boot SB8	Group 4 – AD	Supply Air Boot	V_{ref} = 900 fpm (L/s), V = 447 fpm (L/s)	15
	Total Loss Coefficients				***57***

TABLE A3. Equivalent Length Summary By Sections of the Supply Side of the Installed System Based on ACCA Manual D (Concluded)

Duct Section	Installed Fitting	ACCA Manual D Fitting Number	ACCA Manual D Type of Fitting[a, b]	Parameters	Effective Length[c]
Y8-SB9	Splitter Box Y8 10”x8”x6” (250x200x150 mm)	Group 11	Junction Box	V = 474 fpm (L/s)	46
	Supply Boot SB9	Group 4 – AD	Supply Air Boot	V_{ref} = 900 fpm (L/s), V = 474 fpm (L/s)	17
	Total Loss Coefficients				***63***
SP-Y3	Collar Entry	Group 1 – A	Supply Air Fitting at the AHU		***35***
Y3-Y1	Splitter Box Y3 12”x10”x10” (305x250x250 mm)	Group 11	Junction Box	V = 444 fpm (L/s)	***42***
Y3-Y4	Splitter Box Y3 12”x10”x10” (305x250x250 mm)	Group 11	Junction Box	V = 392 fpm (L/s)	***34***
Y1-SB1	Splitter Box Y1 10”x8”x8” (250x200x200 mm)	Group 11	Junction Box	V = 398 fpm (L/s)	35
	Supply Boot SB1	Group 4 – AD	Supply Air Boot	V_{ref} = 900 fpm (L/s), V = 398 fpm (L/s)	12
	Total Loss Coefficients				***47***
Y1-Y2	Splitter Box Y1 10”x8”x8” (250x200x200 mm)	Group 11	Junction Box	V = 295 fpm (L/s)	***19***
Y2-SB2	Splitter Box Y2 8”x6”x6” (200x150x150 mm)	Group 11	Junction Box	V = 311 fpm (L/s)	22
	Supply Boot SB2	Group 4 – AD	Supply Air Boot	V_{ref} = 900 fpm (L/s), V = 311 fpm (L/s)	7
	Total Loss Coefficients				***29***
Y2-SB3	Splitter Box Y2 8”x6”x6” (200x150x150 mm)	Group 11	Junction Box	V = 214 fpm (L/s)	7
	Supply Boot SB3	Group 4 – AD	Supply Air Boot	V_{ref} = 900 fpm (L/s), V = 214 fpm (L/s)	3
	Total Loss Coefficients				***10***
Y4-SB4	Splitter Box Y4 10”x8”x6” (250x200x150 mm)	Group 11	Junction Box	V = 378 fpm (L/s)	32
	Supply Boot SB4	Group 4 – AD	Supply Air Boot	V_{ref} = 900 fpm (L/s), V = 378 fpm (L/s)	11
	Total Loss Coefficients				***43***
Y4-SB5	Splitter Box Y4 10”x8”x6” (250x200x150 mm)	Group 11	Junction Box	V = 418 fpm (L/s)	38
	Supply Boot SB5	Group 4 – AD	Supply Air Boot	V_{ref} = 900 fpm (L/s), V = 418 fpm (L/s)	13
	Total Loss Coefficients				***51***

[a]Junction Boxes EL values listed in ACCA Manual D Group 11, page A3-25 (some values are linearly interpolated).
[b]Supply Boots values are listed in ACCA Manual D for a reference velocity of 900 fpm (4.6 m/s), and therefore are corrected herein for the corresponding velocity ($EL = EL_{ref}.(V/V_{ref})^2$). [c]Reference Pressure Drop is 0.08 in water/100ft (0.65 Pa/m).

TABLE A4. Total Pressure Calculations By Sections of the Supply Side of the Installed System Based on ACCA Manual D

Duct Section	Duct Element	Flow Rate[a] cfm (L/s)	Duct Size in (mm)	Velocity fpm (m/s)	Installed Duct Length ft (m)	Net Installed Duct Length[a] ft (m)	Fitting Equivalent Length[b] L	Fitting Pressure Drop[c] in water (Pa)	Duct Pressure Drop[d] in water/100ft (Pa/m)	Duct Pressure Drop in water (Pa)	Section Static Pressure Drop in water (Pa)
SP-Y5	Duct	757 (357.3)	14 (356)	708 (3.60)	2.17 (0.66)	2.17 (0.66)			0.090 (0.74)	0.002 (0.49)	
	Fitting	757 (357.3)		708 (3.60)			35	0.028 (6.97)			0.030 (7.46)
Y5–Y6	Duct	298 (140.7)	10 (250)	546 (2.78)	2.67 (0.81)	2.67 (0.81)			0.080 (0.65)	0.002 (0.53)	
	Fitting	298 (140.7)		546 (2.78)			62	0.050 (12.35)			0.052 (12.89)
Y5-Y7	Duct	459 (216.6)	12 (305)	584 (2.97)	12.00 (3.66)	12.00 (3.66)			0.060 (0.49)	0.007 (1.79)	
	Fitting	459 (216.6)		584 (2.97)			71	0.057 (14.15)			0.064 (15.94)
Y6-SB6	Duct	213 (100.5)	8 (200)	610 (3.10)	3.50 (1.07)	1.92 (0.59)			0.140 (1.14)	0.003 (0.67)	
	Fitting	213 (100.5)		610 (3.10)			106	0.085 (21.12)			0.087 (21.79)
Y6-SB7	Duct	85 (40.1)	6 (150)	433 (2.20)	9.17 (2.79)	7.46 (2.28)			0.100 (0.82)	0.007 (1.86)	
	Fitting	85 (40.1)		433 (2.20)			54	0.043 (10.76)			0.051 (12.62)
Y7-Y9	Duct	210 (99.1)	10 (250)	385 (1.96)	6.17 (1.88)	6.17 (1.88)			0.044 (0.36)	0.003 (0.68)	
	Fitting	210 (99.1)		385 (1.96)			33	0.026 (6.58)			0.029 (7.25)
Y7-Y8	Duct	249 (117.5)	10 (250)	457 (2.32)	8.67 (2.64)	8.67 (2.64)			0.060 (0.49)	0.005 (1.30)	
	Fitting	249 (117.5)		457 (2.32)			44	0.035 (8.77)			0.040 (10.06)

TABLE A4. Total Pressure Calculations By Sections of the Supply Side of the Installed System Based on ACCA Manual D (Continued)

Duct Section	Duct Element	Flow Rate[a] cfm (L/s)	Duct Size in (mm)	Velocity fpm (m/s)	Installed Duct Length ft (m)	Net Installed Duct Length[a] ft (m)	Fitting Equivalent Length[b] L	Fitting Pressure Drop[c] in water (Pa)	Duct Pressure Drop[d] in water/100ft (Pa/m)	Duct Pressure Drop in water (Pa)	Section Static Pressure Drop in water (Pa)
Y9-SB10	Duct	132 (62.3)	8 (200)	378 (1.92)	5.50 (1.68)	3.92 (1.19)			0.058 (0.47)	0.002 (0.57)	
	Fitting	132 (62.3)		378 (1.92)			46	0.037 (9.17)			0.039 (9.73)
Y9-SB11	Duct	78 (36.8)	6 (150)	397 (2.02)	11.00 (3.35)	9.30 (2.83)			0.086 (0.70)	0.008 (1.99)	
	Fitting	78 (36.8)		397 (2.02)			47	0.038 (9.37)			0.046 (11.36)
Y8-SB8	Duct	156 (73.6)	8 (200)	447 (2.27)	5.42 (1.65)	3.84 (1.17)			0.080 (0.65)	0.003 (0.76)	
	Fitting	156 (73.6)		447 (2.27)			57	0.046 (11.36)			0.049 (12.12)
Y8-SB9	Duct	93 (43.9)	6 (150)	474 (2.41)	7.50 (2.29)	5.80 (1.77)			0.110 (0.90)	0.006 (1.59)	
	Fitting	93 (43.9)		474 (2.41)			63	0.050 (12.55)			0.057 (14.14)
SP-Y3	Duct	456 (215.2)	12 (305)	581 (2.95)	8.67 (2.64)	8.67 (2.64)			0.060 (0.49)	0.005 (1.30)	
	Fitting	456 (215.2)		581 (2.95)			35	0.028 (6.97)			0.033 (8.27)
Y3-Y1	Duct	242 (114.2)	10 (250)	444 (2.25)	2.17 (0.66)	2.17 (0.66)			0.053 (0.43)	0.001 (0.29)	
	Fitting	242 (114.2)		444 (2.25)			42	0.034 (8.37)			0.035 (8.66)
Y3-Y4	Duct	214 (101.0)	10 (250)	392 (1.99)	21.00 (6.40)	21.00 (6.40)			0.050 (0.41)	0.011 (2.62)	
	Fitting	214 (101.0)		392 (1.99)			34	0.027 (6.77)			0.038 (9.39)

TABLE A4. Total Pressure Calculations By Sections of the Supply Side of the Installed System Based on ACCA Manual D (Concluded)

Duct Section	Duct Element	Flow Rate[a] cfm (L/s)	Duct Size in (mm)	Velocity fpm (m/s)	Installed Duct Length ft (m)	Net Installed Duct Length[a] ft (m)	Fitting Equivalent Length[b] L	Fitting Pressure Drop[c] in water (Pa)	Duct Pressure Drop[d] in water/100ft (Pa/m)	Duct Pressure Drop in water (Pa)	Section Static Pressure Drop in water (Pa)
Y1-SB1	Duct	139 (65.6)	8 (200)	398 (2.02)	19.00 (5.79)	17.42 (5.31)			0.063 (0.51)	0.011 (2.73)	
	Fitting	139 (65.6)		398 (2.02)			47	0.038 (9.37)			0.049 (12.10)
Y1-Y2	Duct	103 (48.6)	8 (200)	295 (1.50)	2.25 (0.69)	2.25 (0.69)			0.034 (0.28)	0.000 (0.06)	
	Fitting	103 (48.6)		295 (1.50)			19	0.015 (3.79)			0.015 (3.84)
Y2-SB2	Duct	61 (28.8)	6 (150)	311 (1.58)	5.00 (1.52)	3.30 (1.01)			0.050 (0.41)	0.002 (0.41)	
	Fitting	61 (28.8)		311 (1.58)			29	0.023 (5.78)			0.025 (6.19)
Y2-SB3	Duct	42 (19.8)	6 (150)	214 (1.09)	8.42 (2.57)	6.71 (2.05)			0.026 (0.21)	0.002 (0.43)	
	Fitting	42 (19.8)		214 (1.09)			10	0.008 (1.99)			0.010 (2.43)
Y4-SB4	Duct	132 (62.3)	8 (200)	378 (1.92)	11.00 (3.35)	9.42 (2.87)			0.060 (0.49)	0.006 (1.41)	
	Fitting	132 (62.3)		378 (1.92)			43	0.034 (8.57)			0.040 (9.98)
Y4-SB5	Duct	82 (38.7)	6 (150)	418 (2.12)	12.17 (3.71)	10.46 (3.19)			0.100 (0.82)	0.010 (2.61)	
	Fitting	82 (38.7)		418 (2.12)			51	0.041 (10.16)			0.051 (12.77)

[a]Net installed duct length is the total installed length minus the elbow that feeds the supply boot, as it is considered an integral part of the boot.
[b]Values obtained from various groups of fittings in ACCA Manual D.
[c]Fitting pressure drop corresponding to the ACCA Manual D Reference Friction Rate of 0.08 in water/100ft (0.65 Pa/m) for all fittings.
[d]Duct pressure drop is provided in ACCA Manual D, Chart 7, page A2-10.

TABLE A5. Local Loss Coefficient Summary By Sections of the Supply Side of the Installed System Based on ASHRAE Fundamentals

Duct Section	Installed Fitting	ASHRAE Fundamentals 2001 Type of Fitting[a, b, c]	Parameters	Local Loss Coefficient
SP-Y5	Collar Entry	Bellmouth, Plenum to Round	r/D = 0	***0.5***
Y5-Y6	Splitter Box Y5 14"x12"x10" (356x305x250 mm)	Tee, Rectangular Main to Round Tap, Branch 10" (250 mm)	Q_2/Q_1 = 0.39	***2.24***
Y5-Y7	Splitter Box Y5 14"x12"x10" (356x305x250 mm)	Tee, Rectangular Main to Round Tap, Branch 12" (305 mm)	Q_3/Q_1 = 0.61	***1.97***
Y6-SB6	Splitter Box Y6 10"x8"x6" (250x200x150 mm)	Tee, Rectangular Main to Round Tap, Branch 8" (200 mm)	Q_3/Q_1 = 0.71	1.43
	Supply Boot SB6	Pyramidal Diffuser, with Wall	L/D_h = 1.0	0.4
	Total Loss Coefficients			***1.83***
Y6-SB7	Splitter Box Y6 10"x8"x6" (250x200x150 mm)	Tee, Rectangular Main to Round Tap, Branch 6" (150 mm)	Q_2/Q_1 = 0.29	2.15
	Supply Boot SB7	Pyramidal Diffuser, with Wall	L/D_h = 1.0	0.4
	Total Loss Coefficients			***2.55***
Y7-Y9	Splitter Box Y7 12"x10"x10" (305x250x250 mm)	Tee, Rectangular Main to Round Tap, Branch 10" (250 mm)	Q_2/Q_1 = 0.46	***2.74***
Y7-Y8	Splitter Box Y7 12"x10"x10" (305x250x250mm)	Tee, Rectangular Main to Round Tap, Branch 10" (250 mm)	Q_2/Q_1 = 0.54	***2.16***
Y9-SB10	Splitter Box Y9 10"x8"x6" (250x200x150 mm)	Tee, Rectangular Main to Round Tap, Branch 8" (200 mm)	Q_3/Q_1 = 0.63	1.63
	Supply Boot SB10	Pyramidal Diffuser, with Wall	L/D_h = 1.0	0.4
	Total Loss Coefficients			***2.03***
Y9-SB11	Splitter Box Y9 10"x8"x6" (250x200x150 mm)	Tee, Rectangular Main to Round Tap, Branch 6" (150 mm)	Q_2/Q_1 = 0.37	1.59
	Supply Boot SB11	Pyramidal Diffuser, with Wall	L/D_h = 1.0	0.4
	Total Loss Coefficients			***1.99***
Y8-SB8	Splitter Box Y8 (10"x8"x6") (250x200x150 mm)	Tee, Rectangular Main to Round Tap, Branch 8" (200 mm)	Q_3/Q_1 = 0.63	1.63
	Supply Boot SB8	Pyramidal Diffuser, with Wall	L/D_h = 1.0	0.4
	Total Loss Coefficients			***2.03***
Y8-SB9	Splitter Box Y8 10"x8"x6" (250x200x150 mm)	Tee, Rectangular Main to Round Tap, Branch 6" (150 mm)	Q_2/Q_1 = 0.37	1.59
	Supply Boot SB9	Pyramidal Diffuser, with Wall	L/D_h = 1.0	0.4
	Total Loss Coefficients			***1.99***
SP-Y3	Collar Entry	Bellmouth, Plenum to Round	r/D = 0	***0.5***
Y3-Y1	Splitter Box Y3 12"x10"x10" (305x250x250 mm)	Tee, Rectangular Main to Round Tap, Branch 10" (250 mm)	Q_2/Q_1 = 0.53	***2.21***
Y3-Y4	Splitter Box Y3 12"x10"x10" (305x250x250 mm)	Tee, Rectangular Main to Round Tap, Branch 10" (250 mm)	Q_2/Q_1 = 0.47	***2.65***

TABLE A5. Local Loss Coefficient Summary By Sections of the Supply Side of the Installed System Based on ASHRAE Fundamentals (Concluded)

Duct Section	Installed Fitting	ASHRAE Fundamentals 2001 Type of Fitting[a, b, c]	Parameters	Local Loss Coefficient
Y1-SB1	Splitter Box Y1 10"x8"x8" (250x200x200 mm)	Tee, Rectangular Main to Round Tap, Branch 8" (200 mm)	$Q_2/Q_1 = 0.57$	1.83
	Supply Boot SB1	Pyramidal Diffuser, with Wall	$L/D_h = 1.0$	0.4
	Total Loss Coefficients			***2.23***
Y1-Y2	Splitter Box Y1 10"x8"x8" (250x200x200 mm)	Tee, Rectangular Main to Round Tap, Branch 8" (200 mm)	$Q_2/Q_1 = 0.43$	***2.71***
Y2-SB2	Splitter Box Y2 8"x6"x6" (200x150x150 mm)	Tee, Rectangular Main to Round Tap, Branch 6" (150 mm)	$Q_2/Q_1 = 0.59$	1.51
	Supply Boot SB2	Pyramidal Diffuser, with Wall	$L/D_h = 1.0$	0.4
	Total Loss Coefficients			***1.91***
Y2-SB3	Splitter Box Y2 8"x6"x6" (200x150x150 mm)	Tee, Rectangular Main to Round Tap, Branch 6" (150 mm)	$Q_2/Q_1 = 0.41$	2.37
	Supply Boot SB3	Pyramidal Diffuser, with Wall	$L/D_h = 1.0$	0.4
	Total Loss Coefficients			***2.77***
Y4-SB4	Splitter Box Y4 10"x8"x6" (250x200x150 mm)	Tee, Rectangular Main to Round Tap, Branch 8" (200 mm)	$Q_3/Q_1 = 0.62$	1.65
	Supply Boot SB4	Pyramidal Diffuser, with Wall	$L/D_h = 1.0$	0.4
	Total Loss Coefficients			***2.05***
Y4-SB5	Splitter Box Y4 10"x8"x6" (250x200x150 mm)	Tee, Rectangular Main to Round Tap, Branch 6" (150 mm)	$Q_2/Q_1 = 0.38$	1.54
	Supply Boot SB5	Pyramidal Diffuser, with Wall	$L/D_h = 1.0$	0.4
	Total Loss Coefficients			***1.94***

[a]Entries values are from Table SD1-1, page 34.48, ASHRAE Fundamentals 2001 (IP).
[b]Splitter Boxes are not reported in ASHRAE Fundamentals 2001 (IP). Values used herein are from Table SR5-11, page 34.65, Rectangular Main to Round Tap, Diverging; the fitting that can best represent a splitter box among all listed fittings.
[c]The types of Supply Boots used in the installed system are not reported in ASHRAE Fundamentals 2001 (IP). Values used herein are from Table SR2-6, page 34.62, Pyramidal Diffuser, with Wall; the fitting that can best represent the supply boots among all listed fittings.

TABLE A6. Total Pressure Calculations By Sections of the Supply Side of the Installed System Based on ASHRAE Fundamentals

Duct Section	Duct Element	Flow Rate[a] cfm (L/s)	Duct Size in (mm)	Velocity fpm (m/s)	Velocity Pressure in water (Pa)	Fully Stretched Duct Length ft (m)	Installed Duct Length ft (m)	Compression Ratio r_c	PDCF[a]	Fitting Loss Coefficient C	Duct Pressure Drop[b] in water/100ft (Pa/m)	Total Pressure Drop in water (Pa)	Section Total Pressure Drop in water (Pa)
SP-Y5	Duct	757 (357.3)	14 (356)	708 (3.60)		2.67 (0.81)	2.17 (0.66)	0.19	2.85		0.260 (2.13)	0.006 (1.40)	
	Fitting	757 (357.3)		708 (3.60)	0.031 (7.76)					0.50		0.016 (3.88)	0.021 (5.28)
Y5–Y6	Duct	298 (140.7)	10 (250)	546 (2.78)		3.00 (0.91)	2.67 (0.81)	0.11	2.10		0.175 (1.43)	0.005 (1.16)	
	Fitting	298 (140.7)		546 (2.78)	0.019 (4.62)					2.24		0.042 (10.35)	0.046 (11.50)
Y5-Y7	Duct	459 (216.6)	12 (305)	584 (2.97)		12.00 (3.66)	12.00 (3.66)	0.00	1.00		0.076 (0.62)	0.009 (2.26)	
	Fitting	459 (216.6)		584 (2.97)	0.021 (5.28)					1.97		0.042 (10.41)	0.051 (12.67)
Y6-SB6	Duct	213 (100.5)	8 (200)	610 (3.10)		4.58 (1.40)	3.50 (1.07)	0.24	3.33		0.456 (3.73)	0.016 (3.98)	
	Fitting	213 (100.5)		610 (3.10)	0.023 (5.76)					1.83		0.042 (10.54)	0.058 (14.52)
Y6-SB7	Duct	85 (40.1)	6 (150)	433 (2.20)		11.00 (3.35)	9.17 (2.79)	0.17	2.64		0.263 (2.15)	0.024 (6.02)	
	Fitting	85 (40.1)		433 (2.20)	0.012 (2.90)					2.55		0.030 (7.39)	0.054 (13.41)
Y7-Y9	Duct	210 (99.1)	10 (250)	385 (1.96)		7.42 (2.26)	6.17 (1.88)	0.17	2.66		0.111 (0.91)	0.007 (1.71)	
	Fitting	210 (99.1)		385 (1.96)	0.009 (2.29)					2.74		0.025 (6.28)	0.032 (7.99)
Y7-Y8	Duct	249 (117.5)	10 (250)	457 (2.32)		9.58 (2.92)	8.67 (2.64)	0.10	1.94		0.114 (0.93)	0.010 (2.45)	
	Fitting	249 (117.5)		457 (2.32)	0.013 (3.22)					2.16		0.028 (6.96)	0.038 (9.42)

TABLE A6. Total Pressure Calculations By Sections of the Supply Side of the Installed System Based on ASHRAE Fundamentals (Continued)

Duct Section	Duct Element	Flow Rate[a] cfm (L/s)	Duct Size in (mm)	Velocity fpm (m/s)	Velocity Pressure in water (Pa)	Fully Stretched Duct Length ft (m)	Installed Duct Length ft (m)	Compression Ratio r_c	PDCF[a]	Fitting Loss Coefficient C	Duct Pressure Drop[b] in water/100ft (Pa/m)	Total Pressure Drop in water (Pa)	Section Total Pressure Drop in water (Pa)
Y9-SB10	Duct	132 (62.3)	8 (200)	378 (1.92)		6.00 (1.83)	5.50 (1.68)	0.08	1.82		0.097 (0.79)	0.005 (1.33)	
	Fitting	132 (62.3)		378 (1.92)	0.009 (2.21)					2.03		0.018 (4.49)	0.023 (5.82)
Y9-SB11	Duct	78 (36.8)	6 (150)	397 (2.02)		11.50 (3.51)	11.00 (3.35)	0.04	1.43		0.120 (0.98)	0.013 (3.30)	
	Fitting	78 (36.8)		397 (2.02)	0.010 (2.44)					1.99		0.020 (4.86)	0.033 (8.15)
Y8-SB8	Duct	156 (73.6)	8 (200)	447 (2.27)		6.50 (1.98)	5.42 (1.65)	0.17	2.64		0.196 (1.60)	0.011 (2.64)	
	Fitting	156 (73.6)		447 (2.27)	0.012 (3.09)					2.03		0.025 (6.27)	0.036 (8.91)
Y8-SB9	Duct	93 (43.9)	6 (150)	474 (2.41)		8.17 (2.49)	7.50 (2.29)	0.08	1.80		0.215 (1.76)	0.016 (4.01)	
	Fitting	93 (43.9)		474 (2.41)	0.014 (3.47)					1.99		0.028 (6.91)	0.044 (10.92)
SP-Y3	Duct	456 (215.2)	12 (305)	581 (2.95)		9.50 (2.90)	8.67 (2.64)	0.09	1.86		0.139 (1.14)	0.012 (3.01)	
	Fitting	456 (215.2)		581 (2.95)	0.021 (5.22)					0.50		0.010 (2.61)	0.023 (5.62)
Y3-Y1	Duct	242 (114.2)	10 (250)	444 (2.25)		2.28 (0.69)	2.17 (0.66)	0.05	1.49		0.082 (0.67)	0.002 (0.44)	
	Fitting	242 (114.2)		444 (2.25)	0.012 (3.05)					2.21		0.027 (6.73)	0.029 (7.18)
Y3-Y4	Duct	214 (101.0)	10 (250)	392 (1.99)		22.33 (6.81)	21.00 (6.40)	0.06	1.59		0.069 (0.56)	0.014 (3.61)	
	Fitting	214 (101.0)		392 (1.99)	0.010 (2.38)					2.65		0.025 (6.31)	0.040 (9.92)

TABLE A6. Total Pressure Calculations By Sections of the Supply Side of the Installed System Based on ASHRAE Fundamentals (Concluded)

Duct Section	Duct Element	Flow Rate cfm (L/s)	Duct Size in (mm)	Velocity fpm (m/s)	Velocity Pressure in water (Pa)	Fully Stretched Duct Length ft (m)	Installed Duct Length ft (m)	Compression Ratio r_c	PDCF[a]	Fitting Loss Coefficient C	Duct Pressure Drop[b] in water/100ft (Pa/m)	Total Pressure Drop in water (Pa)	Section Total Pressure Drop in water (Pa)
Y1-SB1	Duct	139 (65.6)	8 (200)	398 (2.02)		19.67 (5.99)	19.00 (5.79)	0.03	1.33		0.079 (0.64)	0.015 (3.73)	
	Fitting	139 (65.6)		398 (2.02)	0.010 (2.45)					2.23		0.022 (5.47)	0.037 (9.20)
Y1-Y2	Duct	103 (48.6)	8 (200)	295 (1.50)		2.37 (0.72)	2.25 (0.69)	0.05	1.49		0.049 (0.40)	0.001 (0.27)	
	Fitting	103 (48.6)		295 (1.50)	0.005 (1.35)					2.71		0.015 (3.65)	0.016 (3.92)
Y2-SB2	Duct	61 (28.8)	6 (150)	311 (1.58)		5.75 (1.75)	5.00 (1.52)	0.13	2.29		0.119 (0.97)	0.006 (1.48)	
	Fitting	61 (28.8)		311 (1.58)	0.006 (1.49)					1.91		0.011 (2.85)	0.017 (4.33)
Y2-SB3	Duct	42 (19.8)	6 (150)	214 (1.09)		9.33 (2.84)	8.42 (2.57)	0.10	1.97		0.049 (0.40)	0.004 (1.04)	
	Fitting	42 (19.8)		214 (1.09)	0.003 (0.71)					2.77		0.008 (1.96)	0.012 (3.00)
Y4-SB4	Duct	132 (62.3)	8 (200)	378 (1.92)		12.33 (3.76)	11.00 (3.35)	0.11	2.07		0.110 (0.90)	0.012 (3.02)	
	Fitting	132 (62.3)		378 (1.92)	0.009 (2.21)					2.05		0.018 (4.54)	0.030 (7.55)
Y4-SB5	Duct	82 (38.7)	6 (150)	418 (2.12)		13.50 (4.11)	12.17 (3.71)	0.10	1.97		0.183 (1.50)	0.022 (5.56)	
	Fitting	82 (38.7)		418 (2.12)	0.011 (2.70)					1.94		0.021 (5.23)	0.043 (10.79)

[a]Pressure Drop Correction Factors from Figure 8, page 34.8, ASHRAE Fundamentals 2001 (IP).
[b]Duct pressure drop is calculated using Equation 19, page 34.7, ASHRAE Fundamentals 2001 (IP), multiplied by the PDCF. The friction factor in Equation 19 is calculated using Equation 21, and an absolute roughness values of 0.01 ft (3 mm) from Table 1, page 34.7, ASHRAE Fundamentals 2001 (IP).